Available online at www.sciencedirect.com
SCIENCE DIRECT®
Precambrian Research 135 (2004) 79–103
Precambrian Research
www.elsevier.com/locate/precamres

Geochemistry of the Meso- to Neoproterozoic basic–acid rocks from Hunan Province, South China: implications for the evolution of the western Jiangnan orogen

Xiaolei Wang, Jincheng Zhou*, Jiansheng Qiu, Jianfeng Gao

State Key Laboratory for Mineral Deposits Research, Department of Earth Sciences, Nanjing University, Nanjing 210093, PR China

Received 24 June 2003; accepted 20 July 2004

Abstract

The formation and evolution of the Jiangnan orogen at the southeastern margin of the Yangtze Block, South China, are an important and debatable topic. The Meso- to Neoproterozoic basic–acid rocks from Hunan Province record the history of the western Jiangnan orogen in the area. The Mesoproterozoic basalts and diabases from Nanqiao are the typical N-MORB, having very low K_2O, low incompatible HFSE and REE, and depleted ε_{Nd} (T) values (+6.86 to +8.98). They may represent the fragments of an obducted oceanic crust or the relicts of the oceanic crust in a "forearc basin" along an ancient subduction zone, which provides new evidence for the existence of the Jiuling Old Island Arc. The Mesoproterozoic komatiitic basalts from Yiyang are high in Al_2O_3/TiO_2, MgO, Ni and Cr, and are depleted in Nb and Ti. These plume-derived magmas are associated with island-arc tholeiites and exhibit the geochemical characteristics of the arc magma, suggesting that the Mesoproterozoic komatiitic basalts might be the products of the plume–arc interaction. The Neoproterozoic andesitic rocks from Baolinchong, with strong depletions of Nb, Ti and enrichment of LILEs, are of typical island–arc volcanic origin. The Neoproterozoic granites from northeastern Hunan are strongly peraluminous (SP) granites, with high ASI (>1.1) and high CaO/Na_2O ratio (>0.3), suggesting that they might be derived from the partial melting of the psammitic sources in the Mesoproterozoic Lengjiaxi Group. The field geological, chronological, petrographical, geochemical, and isotopic features of these granites indicate that they are the products of post-collisional magmatism related to the breakoff of subducted slab, similar to the andesitic rocks from Baolinchong. The Neoproterozoic basic rocks from the western and central Hunan have the geochemical signatures of rifting basalts, with normalized patterns similar to ocean island basalts (OIB). Their occurrence in intraplate extensional environments is considered as indicators of the rifting of the area. Both the distribution style and field geological evidence of these Neoproterozoic basic rocks are not in line with a mantle plume model. Based on geochemical and petrological studies of the Meso- to Neoproterozoic basic–acid rocks, a preliminary model for the formation and evolution history of the western Jiangnan orogen in the area was put forward.

Keywords: Geochemistry; Proterozoic; Basic–acid rocks; Western Jiangnan orogen; Hunan Province

* Corresponding author. Tel.: +86 25 3686336; fax: +86 25 3686016.
E-mail address: j.c.zhou@public1.ptt.js.cn (J. Zhou).

0301-9268/$ – see front matter © 2004 Elsevier B.V. All rights reserved.
doi:10.1016/j.precamres.2004.07.006

1. Introduction

The Jiangnan orogen, also known as the Jiangnan Oldland and Jiangnan Fold Belt, is a ca. 1500 km long NEE-trending belt at the southeastern margin of the Yangtze Block, South China (Fig. 1). The orogen is the suture belt between the Yangtze and Cathysia blocks in South China (Guo et al., 1980; Chen et al., 1991; Xu et al., 1992; Zhou and Zhu, 1993; Shu et al., 1995). The tectonic evolution of the Jiangnan orogen is an issue of long-standing debate. Guo et al. (1980) proposed that the Jiangnan orogenic belt was the result of the Meso- to Neoproterozoic amalgamation of the Yangtze and Cathysia blocks. However, Hsü et al. (1988) reinterpreted the non-fossiliferous Banxi Group in the Jiangnan orogen as a Mesozoic melange and proposed that Yangtze and Cathysia were collided in the Triassic. Recent geochronological, geochemical and isotopic studies of the granites and ophiolites, however, suggest a Neoproterozoic continental collision between the two blocks (Chen et al., 1991; Xu et al., 1992; Zhou and Zhu, 1993; Shu et al., 1995; Charvet et al., 1996; Li et al., 1997). Recently, it was proposed that the Jiangnan orogen is part of Grenvillian-aged orogens in the world (Li and Mu, 1999; Li et al., 2002b), being formed at ~850 Ma (Zhao and Cawood, 1999; Lu, 2001).

The Jiangnan orogen consists of voluminous Proterozoic basic–acid rocks, which are dominated by strongly peraluminous (SP) granites. Their formations have been considered to be related to the "superplume" event that led to the breakup of the Rodinia supercontinent (Li et al., 1999, 2003a, 2003b). However, the model of a Neoproterozoic superplume beneath the South China is still controversial and remains unsolved (Zhou et al., 2000, 2002, 2004; Yan et al., 2002; Xu, 2002).

This study focuses on investigating the Meso- to Neoproterozoic basic–acid rocks from Hunan Province in the western Jiangnan orogen (HPWJO). They are located between the central and westernmost parts of the Jiangnan orogen, and have been interpreted as the products of magmatism during the process of the evolution of the Jiangnan orogen in the area (Xiao, 1983; Jin and Fu, 1986; Liu and Zhu, 1994; Tang et al., 1997; Chen et al., 1998; Wu et al., 2001; Zheng et al., 2001). Detailed studies on the Proterozoic igneous rocks from Hunan Province are beneficial for making a comparison between the eastern, central and western parts of the Jiangnan orogen, and for understanding the evolution of the orogen. In this paper, we report new analyses for major and trace elements and for Nd, Sr isotopes of the Meso- to Neoproterozoic basic–acid rocks that occurred and/or intrude in the Mesoproterozoic Lengjiaxi Group, Neoproterozoic Banxi Group and Sinian Series in HPWJO. These data place constraints on the tectonic settings of the Precambrian magmatism and on the crustal evolution of the region before and after the assembly of the Yangtze and Cathysia blocks.

2. Regional geology

The Meso- to Neoproterozoic strata in HPWJO comprise two low-grade metamorphic rock series separated by an unconformity, marking the boundary between the Meso- and Neoproterozoic (Fig. 1). The Mesoproterozoic metamorphic rock series (or the Lengjiaxi Group) is distributed in western, eastern and northeastern Hunan Province, and is composed mainly of psammitic to pelitic rocks with flysch rhythm. The Lengjiaxi Group is characterized by the intercalations of pyroclastics and tholeiitic-calc-alkaline lavas metamorphosed in greenschist facies, and constitutes the basement of the Yangtze block in the area. It was strongly deformed and shows tight linear folds and homoclinal inverted folds with a NE-NEE trending fold axis. The age of the group remains unknown, although Liu and Zhu (1994) reported a Pb–Pb isochron age of 1738 ± 87 Ma for group, and Tang et al. (1997) obtained a Sm–Nd whole-rock isochron age of 1330 ± 48 Ma for meta-basic volcanics in the middle part of the group.

The Neoproterozoic metamorphic rock series (or the Banxi Group, equivalent to the Danzhou Group of northern Guangxi) is distributed in western, central and northeastern Hunan Province (Fig. 1), and includes the lower Madiyi Formation and upper Wuqiangxi Formation metamorphosed in lower greenschist facies. The Wuqiangxi Formation contains arkose, carbonaceous slate and marl deposited in a littoral-neritic environment, whereas the Madiyi Formation is composed of purple sandy conglomerates, arkose, pelitic dolomite and turbidite in a continental-neritic deposition environment. The two formations exhibit characteristics of extensional tectonic setting (Liu et al., 1993; Wang and

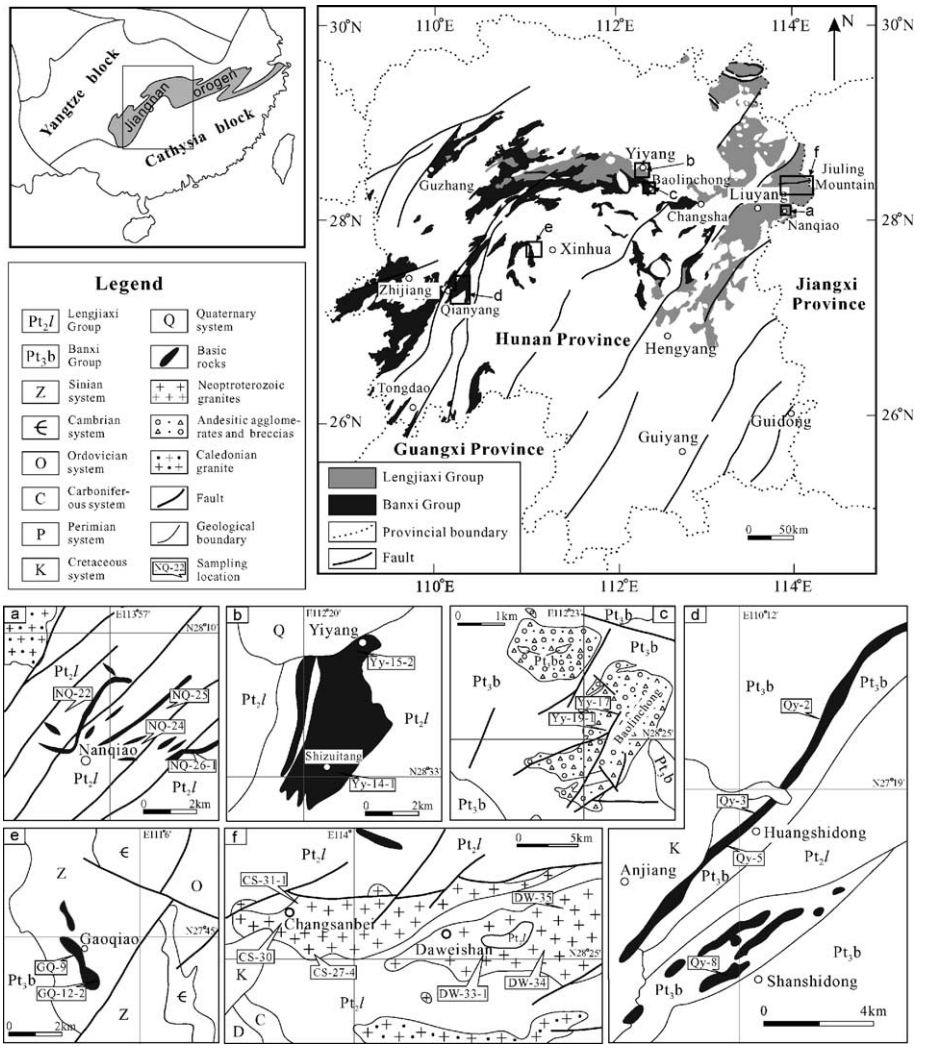

Fig. 1. Sketch geological map of the studied areas in Hunan Province, located in the western Jiangnan orogen (modified after Guo et al., 1984; HRGST, 1976; Zheng et al., 2001, etc.). The upper-left simplified map shows the location of Hunan Province in South China; the upper-right map exhibits the distribution of the Proterozoic strata in Hunan Province. Basalts hosted in the strata of Nanqiao are not illustrated in (a). (a) Nanqiao of Liuyang; (b) Shizuitang of Yiyang; (c) Baolinchong of Yiyang; (d) Shanshidong and Huangshidong of Qianyang; (e) Gaoqiao of Xinhua; and (f) Changsanbei and Daweishan in northeast Hunan.

Li, 2003). The Banxi Group is weakly deformed with broad folds. A depositional break might exist between the Lengjiaxi and Banxi Group (Wang et al., 2003), and the Banxi Group is considered to have developed in the period 820–750 Ma (Wang et al., 2003; Wang and Li, 2003).

The Banxi Group is conformably overlain by the lower Sinian Series which represents the deposits in a rift basin (Chen et al., 1998; Wang and Li, 2003). The lower Sinian Series comprises the Jiangkou, Xiangmeng and Nantuo Formations from bottom to top, and its age ranges from ca. 750 to 680 Ma (Wang et al., 2003; Wang and Li, 2003).

The Meso- to Neoproterozoic basic–acid rocks, with a total outcrop area of ~295 km^2, occur in western, central and northeastern Hunan Province

(Pang, 1983; BGMRHP, 1988). Mesoproterozoic basic rocks in the Lengjiaxi Group occur as lava flows, diabase dykes and layered sills dominantly in the Yiyang–Changsha–Liuyang area (Fig. 1). Neoproterozoic basic (and some intermediate) rocks in the Banxi Group crop out as pyroclastics, lavas and dykes in the Guzhang–Zhijiang–Qianyang–Tongdao area. In addition, some basic volcanic rocks occur in the lower Sinian Series (Jiangkou Formation) scattered in central Hunan Province, especially in the Gaoqiao Village of Xinhua County, Matian village of Wangcheng County and Leishendian Village of Xiangxiang County. Neoproterozoic granites, a part of the westward extension of the Jiuling pluton in Jiangxi Province, are mainly located in northeastern Hunan Province. The basic–acid rocks studied in this work include: (1) the Mesoproterozoic basalts and diabases from the Nanqiao village of Liuyang county, and the komatiitic basalts from Yiyang city; (2) the Neoproterozoic andesitic agglomerates and breccias from the Baolinchong village of Yiyang city, basalts and diabases from Qianyang and Guzhang counties, and the breccia basalts from the Gaoqiao village of Xinhua county in central Hunan; and (3) the Neoproterozoic granites from northeastern Hunan. Simplified stratigraphic column and charts of magmatism in the area are given in Fig. 2. The general geological features of each study area are briefly introduced as follows.

The Mesoproterozoic basic rocks from Nanqiao of Liuyang occur dominantly in the Lengjiaxi Group as layered basalts parallel to the bedding planes of the country rocks. Some basic rocks occur as hypabyssal diabase dykes that intersect the Lengjiaxi Group (Fig. 1a). Contact metamorphic aureoles are absent between the layered basalts and the country rock. Most of the layered basalts are folded together with the meta-sedimentary rocks of the Lengjiaxi Group (HRGST, 1976), suggesting that its age should be Mesoproterozoic. The basalts from Nanqiao of Liuyang yielded a single zircon $^{207}Pb/^{206}Pb$ evaporation age of 1271 ± 2 Ma (Zhou et al., 2003).

The Mesoproterozoic komatiitic basalts are well exposed near the Zishui River in Yiyang city (Fig. 1b). Although these komatiitic basalts have not been dated, they occur in the middle- to upper parts of Lengjiaxi Group, the same horizons as the 1271 ± 2 Ma basalts from Nanqiao of Liuyang (BGMRHP, 1988). The Mesoproterozoic komatiitic basalts are also in conformable or faulted contact with the Mesoproterozoic Lengjiaxi Group (BGMRHP, 1988), suggesting that they might be Mesoproterozoic. The komatiitic basalts from Yiyang have pillow structure, and are associated with the Mesoproterozoic tholeiites (Xiao, 1983; HRGST, 1988; He and Han, 1992).

The Neoproterozoic andesitic agglomerates and breccias from Baolinchong, 15 km south of Yiyang city, occur at the bottom of the Banxi Group (Fig. 1c). These andesitic rocks yielded a SHRIMP U–Pb zircon age of 814 ± 12 Ma (Wang et al., 2003), interpreted as the lower limit of the Banxi Group (Wang et al., 2003).

The Neoproterozoic basic rocks from Qianyang and Guzhang are regarded as the products of contemporaneous magmatism (Liu, 1994; Zheng et al., 2001). They occur in the Wuqiangxi Formation of the Banxi Group and mostly show coincident bedding planes with the country rocks (Fig. 1d). Some diabases intersect the bedding of the country rocks. The contact zone between the basic intrusions and the country rock underwent weak metamorphism, with contact metamorphic aureoles. Recently, Zheng et al. (2001) obtained Sm–Nd whole-rock isochron ages of 868 ± 30 Ma and 855 ± 6 Ma for the basalts and pyroxenite-diabases, respectively, but both data are questionable for their limited variation in Sm/Nd ratios. According to Zheng et al. (2001), the Neoproterozoic basic rocks are uncomfortably overlain by the sandstones of the lower Sinian Series (Chang'an Formation, equivalent to the Jiangkou Formation; see Fig. 2). Therefore, the age of these basic rocks should be younger than the Wuqiangxi Formation and older than the Chang'an Formation, i.e. ca. 760–750 Ma (Fig. 2).

The breccia basalts from Gaoqiao of Xinhua occur in the Jiangkou Formation of the lower Sinian Series (Fig. 1e), and are underlain by the Banxi Group and overlain by the upper Sinian Series glacial deposits (Nantuo Formation) (Chen et al., 1998). Thus, it is clear that its age should be in the range of the lower Sinian Series, i.e.750–680 Ma as mentioned above.

Neoproterozoic granites from northeastern Hunan, with a total outcrop area of $\sim$265.5 km^2, include mainly three plutons: the Changsanbei (76.5 km^2), Daweishan (75 km^2) and Getengling (114 km^2) plutons. Granite samples analyzed in this study were collected from the Changsanbei and Daweishan plutons (Fig. 1f). The

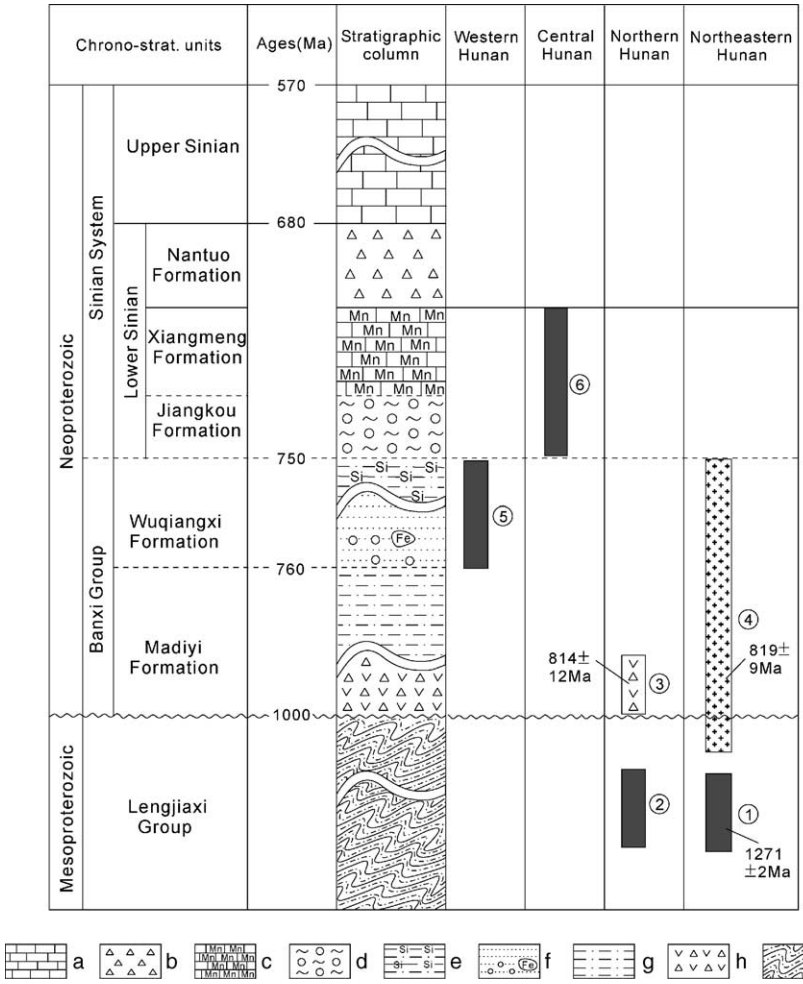

Fig. 2. Simplified stratigraphic column of the Meso- to Neoproterozoic strata and charts of magmatism in Hunan Province, south China (modified after Wang et al., 2003; Wang and Li, 2003). Time scale is after Wang et al. (2003), Wang and Li (2003), Li et al. (2003b) and Zhou et al. (2003). The depositional break between the Mesoproterozoic Lengjiaxi Group and the Neoproterozoic Banxi Group is not shown here. (1) Basalts and diabases from Nanqiao, (2) komatiitic basalts from Yiyang, (3) andesitic rocks from Baolinchong, (4) granites from northeastern Hunan, (5) basic rocks from Qianyang and Guzhang and (6) breccia basalts from Gaoqiao. (a) Carbonate; (b) Glacial diamictite; (c) Mn-bearing Carbonate; (d) Glacial diamictite and conglomerate; (e) Si-bearing slate; (f) Ferruginous pebbly sandstone; (g) Sericite-slate; (h) Continental pyroclastic rock; and (i) Psammitic to pelitic rocks.

granites intrude the metasediments of the Mesoproterozoic Lengjiaxi Group, and are conformably overlain by the sandstones of the Dongmen Formation (equivalent to the Jiangkou Formation) of the lower Sinian Series, as seen in their eastward extension, i.e. the Jiuling pluton of Jiangxi Province (Xu and Zhou, 1992) which yield a zircon SHRIMP U–Pb age of 819 ± 9 Ma (Li et al., 2003a).

3. Petrography

3.1. Basic to intermediate rocks

The Mesoproterozoic basalts and diabases from Nanqiao are grayish green to dark grayish green and show blastodiabastic texture. The matrix, consisting of oligoclase ($An_{22–24}$), exhibits an intergranular texture.

Accessory minerals include chalcopyrite, pyrite, ilmenite and titanite. Nanqiao basic rocks were replaced by tremolite, chlorite and clinozoisite (some display strong carbonation).

The Mesoproterozoic komatiitic basalts from Yiyang show pillow structures. The pillows have a convex upper edge and a flat lower edge, about 0.5–2 m long and 0.2–0.5 m thick and show preferred orientations. Interstices between the pillows with devitrified shells are filled by devitrified and tuffaceous matrix. We did not find any primitive spinifex relicts in the pillowed komatiitic rocks, though they have been reported (Xiao, 1988). The komatiitic basalts were generally replaced by tremolite, sericite, talc and epidote, showing strong alteration. Tremolite (0.5–1.0 mm long and 0.025–0.05 mm wide) is scattered in the altered matrix in radial or bunchy aggregate. The pillow structure of the komatiitic basalts shows a typical characteristic of subaqueous eruptive lavas rather than high MgO cumulates.

The andesites, including the Neoproterozoic andesitic agglomerates and breccias from Baolinchong of Yiyang, show a porphyritic texture with a glassy matrix. The tabular plagioclase phenocrysts are andesine ($An_{35–40}$), and the biotite phenocrysts show dark margins by oxidation.

The predominant phenocrysts in the Neoproterozoic diabases and basalts from Qianyang and Guzhang are augites. The reaction rim is found at the margin of augite phenocrysts. The matrix shows a gabbro-intergranular texture, in which plagioclases are oligoclase ($An_{23–27}$), with some andesine ($An_{36–40}$). These Neoproterozoic basic rocks were replaced by tremolite, chlorite, clinozoisite and calcite due to low-grade metamorphism.

The breccias in the Sinian breccia basalts from Gaoqiao of Xinhua are composed mainly of slaggy basalts with many vesicles, in which the cement was replaced by chlorite, calcite and quartz.

3.2. Acid rocks

The dominant rock types of the Neoproterozoic granites batholith from northeastern Hunan are the biotite-rich and cordierite-bearing granodiorites with minor adamellite, two-mica granite and rare plagiogranite (BGMRHP, 1988). Major rock-forming minerals include plagioclase ($An_{32–37}$), K-feldspar (microperthite and microcline), quartz, biotite and variable amounts of muscovite. The typical aluminum-rich minerals are cordierite and garnet. Accessory minerals include zircon, tourmaline, monazite (HRGST, 1976) and magnetite. Most of the granite samples show weak deformation due to faulting and other tectonothermal events, represented by flaser and stretching quartz grains, weak preferred orientation of quartz, biotite and muscovite having wavy extinction under microscope. Some samples of granites with cataclasis and recrystallization show an obvious gneissic texture. The plutons contain various enclaves which are dominantly mica-rich. The angular enclaves, having a composition similar to that of the wall rocks, occur at the protruding part of the pluton, and the magmatogenic microgranitoid enclaves were also reported (Xu, 1989).

4. Analytical techniques

Major elements were determined by the conventional wet-chemistry method at the Central Laboratory of Department of Earth Sciences, Nanjing University (NJU) with procedures similar to those reported earlier (Liu et al., 1999; Huang et al., 2002). Five samples (NQ-24, NQ-26-1, CS-30, DW-33-1 and DW-34) were analyzed for major elements with an analytical precision less than 1%, using a VF-320 X-ray fluorescence spectrometer (XRF) at the Center of Modern Analysis, NJU, following the procedures described by Franzini et al. (1972).

Rare earth and other trace elements were analyzed using ICP-AES (JY38S) and ICP-MS (Finnigan MAT-Element 2) machines housed at the State Key Laboratory for Mineral Deposits Research, NJU. Procedures for ICP-AES are similar to those of Liu et al. (1999) and Zhu et al. (2001), with a relative accuracy of 5–10%, and that for ICP-MS similar to Zhou et al. (2004). The American USGS, Japanese JGS and Chinese IGGE standards were used for monitoring the quantity of analyses throughout the analytical processes for ICP-MS. Precisely weighted 50 mg sample powders were dissolved in Teflon bombs using $HF + HNO_3$ mixture. An internal standard solution containing the single element Rh was used to monitor signal drift during counting. Analytical precision for most elements by ICP-MS is better than 5%.

Sm–Nd and Rb–Sr isotopic compositions of all samples were determined at the Isotope Laboratory, Institute of Geology and Geophysics, Chinese Academy of Sciences, using MAT-261 and MAT-260 mass spectrograph. The analytical details are given in Shen et al. (1997, 2002). Analytical precisions of Sm/Nd and Rb/Sr ratios both are accurate to less than 0.5–1%.

5. Geochemistry

Major and trace element data are listed in Table 1, and the Sm–Nd and Rb–Sr isotopic data are presented in Table 2. Totals for major element oxides are recalculated to 100% volatile free in plotting. The volcanic rock types in HPWJO include basalts, basaltic andesites, trachybasalts, basaltic trachyandesites with lesser andesites as shown on SiO_2 versus $Na_2O + K_2O$ (TAS) and Nb/Y versus Zr/TiO_2 diagrams (Figs. 3 and 4). Both diagrams indicate that the Mesoproterozoic basic rocks ($\delta < 3.7$) and the Neoproterozoic breccia basalts are sub-alkaline basalts, whereas other Neoproterozoic samples ($\delta > 3.7$) with normative nepheline (sample QY-3, QY-5 and QY-8) are classified as alkaline basalts. The andesitic agglomerates and breccias ($\delta < 3.7$) from Baolinchong of Yiyang belong to calc-alkaline series. Evidently, the granites with high normative corundum (2.69–3.80 wt%, Table 1) and ASI (1.19–1.32, Table 1) from northeastern Hunan are strongly peraluminous granites (Fig. 5).

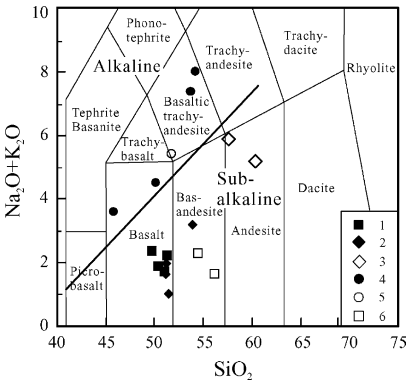

Fig. 3. TAS diagram for the Meso- to Neoproterozoic basic rocks from Hunan Province (after Maitre et al., 1989). (1) Basalts, Nanqiao, (2) komatiitic basalts, Yiyang, (3) andesitic agglomerates and breccias, Baolinchong, (4) diabases and basalts, Qianyang, (5) Basalts, Guzhang and (6) breccia basalts, Gaoqiao.

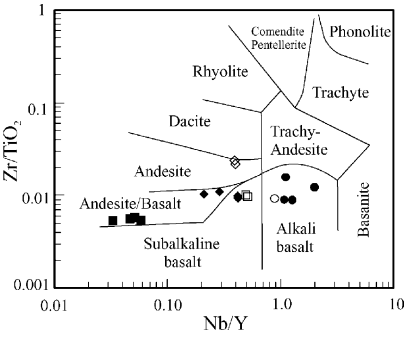

Fig. 4. Zr/TiO_2–Nb/Y diagram for the Meso- to Neoproterozoic basic rocks from Hunan Province (after Winchester and Floyd, 1977). *Note*: Zr is calculated in wt%. Symbols as in Fig. 2.

Geochemical characteristics of these Meso- to Neoproterozoic basic–acid rocks will be further discussed later based on some immobile major element oxides (MgO, Al_2O_3 and TiO_2), compatible elements (Ni, Cr), HFSEs (Nb, Th, Ta, Zr and Hf) and REEs (except Eu) to minimize the effects of metamorphism and alteration.

5.1. Basalts and diabases from Nanqiao

Basalts and diabases from Nanqiao of Liuyang are tholeiitic with especially low K_2O contents (0.10–0.22 wt%), high CaO, low FeO^*/MgO ratios and a few normative quartz. Their REE patterns (Fig. 6a), similar to those of the typical N-MORB, display obvious LREE depletion [$(La/Yb)_N = 0.39–0.69$, $(Gd/Yb)_N = 0.71–0.78$] with weak Eu negative anomalies ($Eu/Eu^* = 0.79–0.94$). Th

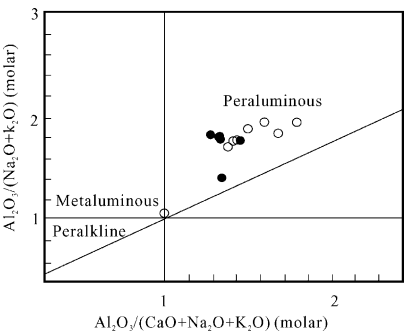

Fig. 5. Diagram of A/NK vs. A/CNK for the Neoproterozoic granites from northeast Hunan (after Maniar and Piccolli, 1989). Solid circle, this study; open circle, data from Wu et al. (2001).

Table 1
Major (wt%), trace and rare earth element (ppm) analyses for the Meso- to Neoproterozoic basic–acid rocks from Hunan Province

	Nanqiao (Mesop.)[a]				Yiyang (Mesop.)[a]				Yiyang (Neop.)[a]	
	Basalt[b]			Diabase[b]	Komatiitic basalt[b]				Andesite[b]	Andesitic agglomerate[b]
	NQ-22[c] 1[d]	NQ-24[c] 2[d]	NQ-25[c] 3[d]	NQ-26-1[c] 4[d]	Yy-14-1[c] 5[d]	Yy-15-2[c] 6[d]	Yyb-1[c] 7[d]	Yyb-2[c] 8[d]	Yy-17[c] 9[d]	Yy-19-1[c] 10[d]
Major elements (wt%)										
SiO_2	49.50	48.31	49.08	49.68	51.96	49.24	51.06	50.83	58.04	55.2
TiO_2	0.68	0.46	0.61	0.76	0.46	0.47	0.55	0.53	0.66	0.69
Al_2O_3	13.40	17.78	13.90	13.81	12.71	11.34	12.18	11.67	16.62	18.21
Fe_2O_3	2.53	8.58[e]	2.87	11.63[e]	0.97	2.47	1.95	2.45	5.38	4.21
FeO	8.16		7.44		7.16	6.96	7.88	7.27	1.73	2.22
MnO	0.20	0.15	0.18	0.21	0.14	0.16	0.15	0.15	0.12	0.12
MgO	7.53	6.89	7.81	7.15	10.85	13.27	13.70	13.76	4.25	4.94
CaO	13.21	12.24	13.57	11.38	8.97	10.23	10.59	10.99	4.14	4.43
Na_2O	1.57	2.09	1.68	2.02	2.95	1.61	0.49	1.11	3.01	3.52
K_2O	0.13	0.22	0.18	0.10	0.14	0.31	0.54	0.49	2.01	2.15
P_2O_5	0.09	<0.01	0.09	0.03	0.07	0.08	0.08	0.08	0.18	0.19
LOI	2.32	2.31	2.43	1.66	2.98	3.51	–	–	3.17	3.45
Total	99.32	99.03	99.84	98.43	99.36	99.67	99.17	99.33	99.31	99.33
Al_2O_3/TiO_2	19.71	38.65	22.79	18.17	27.63	24.13	22.15	22.02	25.18	26.39
CaO/Na_2O	8.41	5.86	8.08	5.63	3.04	6.35	21.61	9.90	1.38	1.26
δ	0.44	1.00	0.57	0.67	1.07	0.59	0.13	0.33	1.68	2.64
Trace elements (ppm)										
La	1.77	2.48	1.77	2.22	6.52	9.35	7.26	6.86	36.6	73.1
Ce	4.25	2.80	3.40	4.63	13.6	16.4	14.9	13.0	61.8	115
Pr	0.75	0.69	0.61	0.83	1.99	2.32	1.96	1.74	7.10	10.8
Nd	4.16	3.26	3.28	4.50	7.28	9.03	7.88	7.22	28.4	43.3
Sm	1.55	1.26	1.21	1.84	1.71	2.09	2.01	1.78	5.26	6.88
Eu	0.63	0.52	0.51	0.66	0.36	0.57	0.67	0.72	1.27	1.40
Gd	3.02	2.21	2.40	3.43	2.00	2.35	3.39	3.51	4.09	4.84
Tb	0.56	0.41	0.44	0.60	0.32	0.38	0.29	0.35	0.52	0.59
Dy	4.51	3.18	3.45	4.53	2.19	2.54	2.28	2.25	2.95	3.42
Ho	1.04	0.83	0.79	1.26	0.46	0.54	0.50	0.45	0.60	0.71
Er	2.90	2.39	2.21	3.91	1.22	1.43	1.34	1.31	1.37	1.70
Tm	0.45	0.40	0.35	0.53	0.20	0.24	0.20	0.17	0.22	0.28

Yb	3.22	2.58	2.55	3.87	1.40	1.61	1.19	1.22	1.50	1.91
Lu	0.48	0.39	0.39	0.61	0.22	0.25	0.24	<0.10	0.22	0.29
Rb	5.1	15.3	6.2	4.3	5.5	11.2	23	17	75.7	79.5
Sr	67.8	111	74.5	70.2	81.9	75.8	81	77	440	291
Y	27.7	19.5	21.6	25.5	12.2	14.6	11.3	11.3	15.3	17.2
Sc	30.8	34.5	30.8	43.3	27	27.5	18	20	17.3	18.4
Co	56.4	35.9	53.3	40.2	74.0	60.0	42.0	37.0	21.2	25.8
Ni	82	110	97	98	330	338	293	232	59	46
Cr	156	441	158	149	970	996	842	863	142	146
Zr	39.4	25.3	33.9	45.0	52.0	50.0	53	54	156	174
Hf	1.14	0.72	1.01	1.24	1.13	1.20	–	–	3.91	4.48
Ba	28	16.2	66	12.6	98	151	201	100	487	453
Nb	1.31	0.64	1.27	1.29	3.7	3.2	5	5	6.44	7.16
Ta	0.11	0.07	0.13	0.12	0.15	0.15	–	–	0.54	0.61
Th	0.18	0.29	0.10	0.62	2.46	2.41	5	4.3	10.9	11.9
U	0.24	0.12	0.24	0.18	0.29	0.32	–	–	1.57	1.85
Zr/Nb	30.08	39.53	26.69	34.88	14.05	15.63	10.60	10.80	24.22	24.30
Nb/La	0.74	0.26	0.72	0.58	0.57	0.34	0.69	0.73	0.18	0.10
Eu/Eu*	0.88	0.94	0.90	0.79	0.59	0.78	0.78	0.86	0.81	0.70
Nb/Nb*	0.78	0.26	0.95	0.34	0.27	0.21	0.20	0.23	0.10	0.08
Ti/Ti*	0.71	0.62	0.80	0.72	0.77	0.59	0.52	0.48	0.42	0.39
$(La/Yb)_N$	0.39	0.69	0.50	0.41	3.34	4.17	4.38	4.03	17.50	27.45
$(Gd/Yb)_N$	0.78	0.71	0.78	0.73	1.18	1.21	2.36	2.38	2.26	2.10

Table 1 (*Continued*)

	Northeastern Hunan (Neop.)[a]						Qianyang and Guzhang (Neop.)[a]					Gaoqiao (Neop.)[a]	
	Two-mica granite[b]	Plagio-granite[b]	Grano-diorite[b]				Diabase[b]			Basalt[b]	Diabase[b]	Breccia basalt[b]	
	CS-27-4[c] 12[d]	CS-30[c] 13[d]	CS-31-1[c] 14[d]	DW-33-1[c] 15[d]	DW-34[c] 16[d]	DW-35[c] 17[d]	Qy-2[c] 18[d]	Qy-3[c] 19[d]	Qy-5[c] 20[d]	Qy-8[c] 21[d]	GZ-38[c] 22[d]	GQ-9[c] 23[d]	GQ-12-2[c] 24[d]
Major elements (wt%)													
SiO_2	69.84	72.72	70.49	68.25	68.26	68.76	47.58	48.86	50.74	43.52	49.60	52.55	51.46
TiO_2	0.43	0.29	0.52	0.67	0.69	0.57	1.75	2.69	2.19	2.43	1.75	4.08	4.85
Al_2O_3	13.79	12.94	14.25	14.35	14.49	14.62	12.24	13.72	13.81	13.20	14.66	10.11	10.93
Fe_2O_3	0.69	0.40	4.20[e]	5.80[e]	5.75[e]	1.62	2.69	1.29	1.87	2.22	2.90	5.86	6.25
FeO	2.87	2.38				3.01	8.40	8.67	8.58	8.64	7.97	6.02	5.83
MnO	0.12	0.04	0.06	0.17	0.09	0.08	0.18	0.18	0.16	0.17	0.16	0.17	0.12
MgO	1.29	0.87	1.30	1.73	1.86	1.69	11.11	3.37	2.46	10.22	5.87	7.33	6.91
CaO	1.45	0.66	1.93	2.03	2.05	2.31	6.26	5.00	5.37	10.55	7.46	5.04	5.19
Na_2O	2.08	2.33	2.83	2.41	2.45	2.64	3.15	5.53	5.87	1.85	4.52	0.31	1.07
K_2O	4.07	4.99	3.12	3.72	3.70	3.42	1.15	1.19	1.64	1.59	0.69	1.25	1.12
P_2O_5	0.17	0.14	0.10	0.09	0.12	0.14	0.31	0.44	0.88	0.58	0.27	0.86	0.78
LOI	2.57	1.54	1.20	0.87	0.92	1.02	5.02	8.37	5.98	4.96	3.60	5.73	4.82
Total	99.37	99.3	100.00	100.09	100.38	99.88	99.84	99.31	99.55	99.93	99.45	99.31	99.33
Al_2O_3/TiO_2	32.07	44.62	27.40	21.42	21.00	25.65	6.99	5.10	6.31	5.43	8.38	2.48	2.25
CaO/Na_2O	0.70	0.28	0.68	0.84	0.84	0.88	1.99	0.90	0.91	5.70	1.65	16.26	4.85
Ne							0.00	1.24	2.02	2.06	0.00	0.00	0.00
C	3.80	2.86	2.94	2.87	2.99	2.69							
δ							4.04	7.71	7.29	22.76	4.11	0.25	0.57
ASI	1.32	1.24	1.23	1.23	1.23	1.19							
Trace elements (ppm)													
La	30.9	34.9	28.7	33.9	33.0	36.5	28.8	41.6	62.1	55.7	27.5	35.9	38.1
Ce	61.3	67.7	61.5	70.4	63.6	68.0	52.9	79.2	120	103	51.5	84.9	92.6
Pr	6.83	7.97	7.21	8.75	7.99	8.24	6.36	9.58	14.0	11.4	6.23	14.4	15.7
Nd	27.3	31.1	27.0	31.6	30.5	32.3	26.5	38.7	58.6	48.0	25.6	57.6	66.0
Sm	5.66	6.63	5.75	7.00	5.64	6.69	5.15	7.88	11.4	8.81	5.33	15.1	16.8
Eu	0.99	0.80	1.14	1.29	0.99	1.07	1.48	2.22	2.79	2.44	1.54	4.60	5.16
Gd	4.96	5.72	5.81	8.14	6.76	6.38	4.71	7.40	10.2	7.36	5.11	14.8	16.4
Tb	0.69	0.69	0.78	1.43	0.84	0.92	0.63	0.99	1.37	0.94	0.68	1.80	1.99
Dy	4.07	3.67	5.24	11.5	5.73	5.77	3.80	5.66	7.90	5.19	4.02	8.77	9.81
Ho	0.80	0.66	1.16	3.04	1.25	1.17	0.72	1.09	1.52	0.95	0.77	1.47	1.63
Er	1.93	1.49	3.23	10.2	3.68	2.90	1.66	2.50	3.49	2.00	1.77	2.69	3.03
Tm	0.31	0.23	0.47	1.59	0.53	0.44	0.23	0.37	0.50	0.27	0.26	0.38	0.42

Yb	2.15	1.55	2.91	11.5	3.00	3.08	1.52	2.38	3.18	1.58	1.70	1.75	1.94
Lu	0.31	0.23	0.44	1.66	0.48	0.45	0.22	0.35	0.45	0.21	0.25	0.25	0.26
Rb	162	208	132	182	173	170	27.5	18.3	41.1	21.9	9.5	46.8	43.0
Sr	76.1	48.9	86.9	88.9	73.2	87.3	356	390	302	942	510	116	108
Y	21.1	17.9	26.2	71.8	29.3	31.2	17.9	27.4	37.6	22.8	19.6	34.5	37.1
Sc	9.34	5.48	9.97	17.5	13.8	11.9	18.7	22.8	14.2	18.3	24.1	14.9	17.4
Co	1.5	5.4	10.7	14.8	14.4	13	71.2	11.8	17.1	57.9	34.4	39.7	40.2
Ni	17.4	14.9	25.4	36.1	38.9	21.9	271	21.1	8.2	176	74.8	159	160
Cr	90.6	34.0	50.8	77.5	86.7	70.2	313	7.6	4.5	176	141	151	176
Zr	161	111	208	182	157	224	161	246	352	305	166	426	485
Hf	4.18	3.13	4.99	5.10	5.30	5.65	3.49	4.60	6.83	4.96	3.16	9.30	10.8
Ba	417	299	336	349	372	348	1018	397	601	934	411	466	455
Nb	8.72	8.96	8.26	10.4	10.1	10.5	20.8	37.7	45.2	49.8	18.7	18.1	20.1
Ta	1.00	1.10	0.86	1.15	1.14	1.26	1.66	3.06	3.69	4.28	1.50	1.05	1.20
Th	8.58	13.9	11.2	14.8	14.1	11.3	4.27	5.77	8.91	5.91	4.8	2.13	2.40
U	1.77	4.93	2.90	2.90	2.66	2.69	0.70	1.15	1.91	1.45	0.80	0.60	0.57
Zr/Nb	18.46	12.39	25.18	17.50	15.54	21.33	7.74	6.53	7.79	6.12	8.88	23.54	24.13
Nb/La	0.28	0.26	0.29	0.31	0.31	0.29	0.72	0.91	0.73	0.89	0.68	0.50	0.53
Eu/Eu*	0.56	0.39	0.60	0.52	0.49	0.49	0.90	0.87	0.77	0.90	0.89	0.93	0.94
Nb/Nb*	0.17	0.12	0.13	0.13	0.13	0.16	0.63	0.82	0.65	0.93	0.54	0.66	0.67
Ti/Ti*	0.28	0.19	0.29	0.29	0.37	0.31	0.97	0.97	0.60	0.83	0.91	0.72	0.77
$(La/Yb)_N$	10.31	16.15	7.07	2.11	7.89	8.50	13.59	12.54	14.01	25.29	11.60	14.71	14.09
$(Gd/Yb)_N$	1.91	3.05	1.65	0.59	1.86	1.71	2.56	2.57	2.65	3.85	2.49	7.00	6.99

Mesop., Mesoproterozoic; Neop., Neoproterozoic; Ne, normative nepheline; C, normative corundum; δ, Rittmann index; ASI, molecular ratio of $Al_2O_3/(CaO + Na_2O + K_2O)$; –, not determined.

[a] Location.

[b] Rock type.

[c] Sample.

[d] Number.

[e] Total ion as Fe_2O_3.

Table 2
Sm–Nd and Rb–Sr isotopic data for the Meso- to Neoproterozoic basic–acid rocks from Hunan Province

No.	Sample	Age (Ma)	Sm (ppm)	Nd (ppm)	$^{147}Sm/^{144}Nd$	$^{143}Nd/^{144}Nd$	$\pm2\sigma$ (10^{-6})	εNd (T)	TDM (Ma)
1	NQ-22	1271	1.76	3.77	0.2818	0.513699	15	6.86	1304
2	NQ-25	1271	1.51	3.22	0.2832	0.513819	14	8.98	1133
3	Yy-14-1	1271	1.84	7.23	0.1543	0.512364	11	1.56	1734
4	Yy-15-2	1271	2.01	8.12	0.1501	0.512339	9	1.76	1718
5	Yy-17	814	4.10	22.6	0.1098	0.512079	9	−1.86	1636
6	Yy-19-1	814	6.23	39.4	0.0956	0.511965	8	−2.60	1696
7	CS-27-4	819	5.76	27.7	0.1258	0.512166	8	−1.78	1634
8	CS-30	819	6.27	28.6	0.1326	0.512164	15	−2.54	1695
9	DW-35	819	6.48	30.3	0.1294	0.512139	10	−2.69	1707
10	QY-2	755	5.06	23.9	0.1278	0.512338	8	0.80	1372
11	QY-3	755	6.32	29.6	0.1293	0.512316	10	0.23	1418
12	QY-5	755	10.0	47.5	0.1273	0.512311	15	0.32	1411
13	QY-8	755	8.29	43.7	0.1148	0.512370	11	2.69	1219
14	GZ-38	755	4.95	22.9	0.1307	0.512359	11	0.83	1361
15	GZb-2	755	3.91	17.5	0.1353	0.512310	28	−0.47	1475
16	GZb-3	755	7.14	32.8	0.1318	0.512346	21	0.57	1390
17	GZb-4	755	6.78	32.7	0.1254	0.512340	9	1.07	1350

			Rb (ppm)	Sr (ppm)	$^{87}Rb/^{86}Sr$	$^{87}Sr/^{86}Sr$	$\pm2\sigma(10^{-6})$	$(^{87}Sr/^{86}Sr)_i$
1	NQ-22	1271	2.11	66.57	0.0917	0.710942	13	0.709
2	NQ-25	1271	19.84	74.08	0.7734	0.710063	20	0.696
3	Yy-14-1	1271	6.80	82.91	0.2368	0.712890	18	0.709
4	Yy-15-2	1271	13.28	76.80	0.4997	0.712680	20	0.704
5	Yy-17	814	87.88	403.0	0.6299	0.712406	28	0.705
6	Yy-19-1	814	78.86	304.0	0.7494	0.712863	14	0.704
7	CS-27-4	819	163.8	73.00	6.5300	0.786070	13	0.710
8	CS-30	819	203.2	45.94	12.940	0.839865	23	0.688
9	DW-35	819	172.6	81.51	6.1600	0.782549	18	0.710
10	QY-2	755	27.64	357.8	0.2231	0.708233	20	0.706
11	QY-3	755	16.47	396.3	0.1200	0.708290	20	0.707
12	QY-5	755	39.98	307.2	0.3758	0.709171	20	0.705
13	QY-8	755	51.96	973.5	0.1541	0.707583	20	0.706
14	GZ-38	755	9.10	534.9	0.0492	0.712095	25	0.712

Note: Sample No. 15, 16 and 17: from Liu (1994), others: this study. The komatiitic basalts from Yiyang are hosted in the same horizon as the 1271 ± 2 Ma basalts from Nanqiao of Liuyang (BGMRHP, 1988), maybe 1271 Ma is relatively suitable for the Nanqiao basalts. The 760–750 Ma basic rocks from Qianyang and Guzhang are calculated at 755 Ma. Granites from Notheaste Hunan are similar in age to the Jiuling Pluton (Li et al., 2003a, 2003b). Age for the andesitic rocks from Baolinchong is after Wang et al. (2003).

contents (0.18–0.62 ppm) of the Nanqiao basic rocks are relatively higher than those of the typical N-MORB, far lower than the average values of crustal gabbros (3.1 ppm; Haack, 1983), suggesting that crustal contamination may not be important to the Nanqiao basic rocks even if it might exist. Their Zr/Nb ratios (26.75–39.65) are close to those of the depleted mantle (Zr/Nb = ∼30). Some incompatible HFSE, such as Nb, Zr, Hf and Ti, in these rocks are lower than those of N-MORB (Fig. 7a), which may be related to their especially low K_2O, exhibiting typical features of N-MORB. Initial $^{87}Sr/^{86}Sr$ ratios of the Nanqiao basalts vary from 0.696 to 0.709 (Table 2), suggesting that the sources were depleted, though the Rb–Sr isotopic system might have been disturbed by low-grade regional metamorphism. The high ε_{Nd} (T) values (+6.86 to +8.98) (Table 2) of these basic rocks indicate their much depleted mantle sources.

5.2. Komatiitic basalts from Yiyang

Komatiitic basalts from Yiyang have intermediate SiO_2 contents (49.24–51.96 wt%), and have Al_2O_3 contents between 11.34 and 12.71 wt%, with low

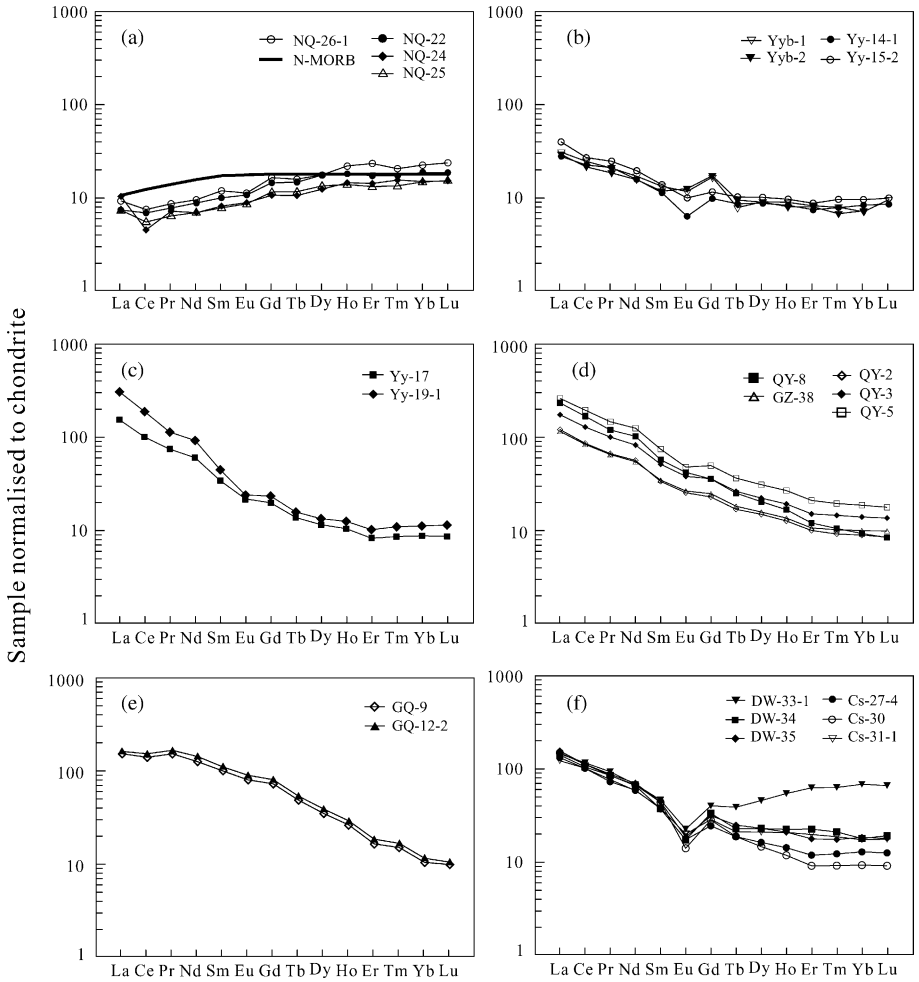

Fig. 6. Chondrite-normalized REE patterns of the Meso- to Neoproterozoic basic–acid rocks from Hunan Province. Chondrite-normalization values and N-MORB data are from Sun and McDonough (1989). (a) Basalts and diabases from Nanqiao, (b) komatiitic basalts from Yiyang, (c) andesitic agglomerates and breccias from Baolinchong, (d) diabases and basalts from Qianyang and Guzhang, (e) breccia basalts from Goaqiao, and (f) granites from northeastern Hunan.

TiO_2 (0.46–0.55 wt%) and high Al_2O_3/TiO_2 ratios (between 22.02 and 27.63). The Nd model ages (T_{DM}) are between 1718 and 1734 Ma, and the ε_{Nd} (T) values are from +1.56 to +1.76, suggesting that the magmas were derived from a slightly depleted mantle. Two geochemical features of these basalts are noticeable. First, they have high MgO (10.85–13.76 wt%), Al_2O_3/TiO_2 (comparable to chondrite), Ni and Cr (232–338 ppm and 842–995.8 ppm, respectively) contents, similar to other komatiitic basalts from the Abitibi Greenstone Belt (Wyman, 1999) and the Northern Superior Province greenstone belt (Hollings and Wyman, 1999; Hollings et al., 1999). They are different from the SHMB (Sensarma et al., 2002) which are related to subduction in their normal SiO_2, and are different from the high-Mg basalts formed in extension-dominated settings (Mattioli et al., 2000) in their high Al_2O_3/TiO_2 ratios. A sub-continental mantle plume is a preferred source for such high temperature and high-Mg komatiitic magmas (Nisbet et al., 1993). Second, the komatiitic basalts exhibit geochemical signatures of island-arc basalts with clear Nb and Ti troughs (Fig. 7b; $Nb/Nb^* = 0.20–0.27$, $Ti/Ti^* = 0.48–0.77$), enriched Th (2.41–5 ppm) in their primitive

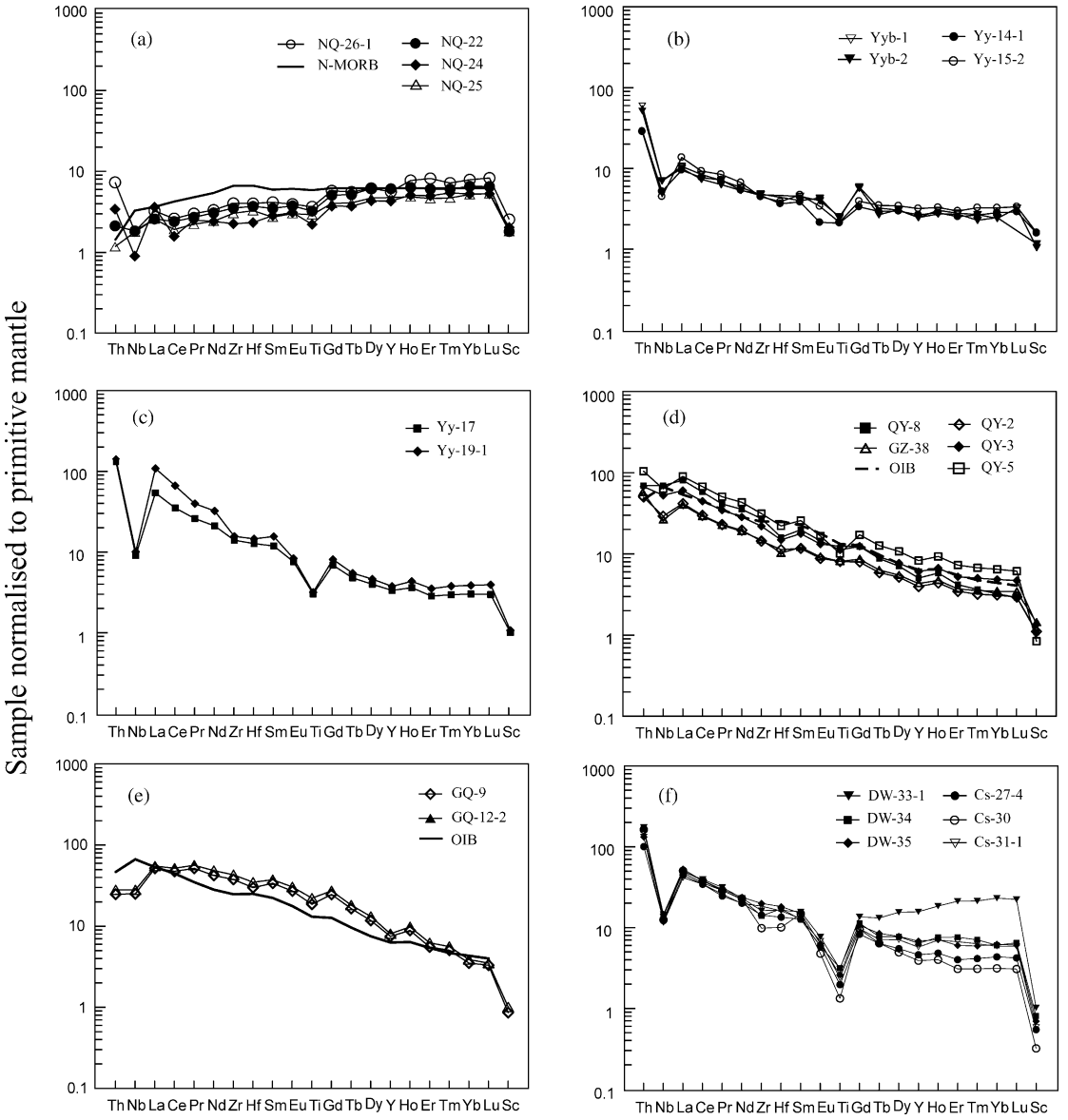

Fig. 7. Primitive mantle-normalized trace element patterns for Meso- to Neoproterozoic basic–acid rocks from Hunan Province. Primitive mantle and ocean island basalt (OIB) data are from Sun and McDonough (1989). (a) Basalts and diabases from Nanqiao, (b) komatiitic basalts from Yiyang, (c) andesitic agglomerates and breccias from Baolinchong, (d) diabases and basalts from Qianyang and Guzhang, (e) breccia basalts from Goaqiao, and (f) granites from northeastern Hunan.

mantle-normalized patterns of trace elements. They are enriched LREE [Fig. 6b; $(La/Yb)_N = 3.34–4.38$, $(Gd/Yb)_N = 1.18–2.38$] and intermediate Eu negative anomalies ($Eu/Eu^* = 0.60–0.86$). According to the geochemical screens (listed here in parentheses) of trace elements for Precambrian basalts (Condie, 1989), the komatiitic basalts should be also classified as the island-arc volcanics for their Nb/La = 0.34–0.57 (<0.8), Hf/Ta = 7.59–8.11 (>5), La/Ta = 43.76–63.17 (>15), Ti/Y = 194–226 (<350), Th/Yb = 1.5–1.76 (>0.1), Th/Nb = 0.66–0.75 (>0.07) and Hf/Th = 0.46–0.5 (<8).

5.3. Andesitic agglomerates and breccias from Baolinchong

Volcanic agglomerates and breccias from Baolinchong of Yiyang are andesitic with low MgO and CaO (4.25–4.94 wt% and 4.14–4.43 wt%, respectively), high Na_2O and Al_2O_3 (3.01–3.52 wt% and 16.62–18.21 wt%, respectively). REE patterns of these andesitic rocks show strong enriched LREE [Fig. 6c; $(La/Yb)_N = 17.54–27.45$; $(Gd/Yb)_N = 2.09–2.26$] and intermediate Eu negative anomalies ($Eu/Eu^* = 0.70–0.81$), suggesting the fractional crystallization of plagioclase. Clear Nb and Ti troughs occur in the primitive mantle-normalized patterns of trace element (Fig. 7c; $Nb/Nb^* = 0.08–0.10$ and $Ti/Ti^* = 0.39–0.42$, respectively). Moreover, the enrichments of Th, La, Sm and Nd, and the low ε_{Nd} (T) values (between −1.86 and −2.60) suggest that these rocks are derived from subduction-related lavas.

5.4. Basalts and diabases from Qianyang and Guzhang

Neoproterozoic basalts and diabases from Qianyang and Guzhang have high TiO_2 (1.75–2.69 wt%), moderate Al_2O_3 (12.24–14.66 wt%) and low Al_2O_3/TiO_2 ratios (5.10–6.99). MgO contents are relatively low (2.46–11.11 wt%) and Ni and Cr (8.2–271 ppm and 4.53–312.9 ppm, respectively) increase with increasing MgO, indicating the possibility of the fractional crystallization of olivine. LREE are highly enriched [$(La/Yb)_N = 11.62–25.26$, $(Gd/Yb)_N = 2.49–3.85$] relative to HREE, with weak negative Eu anomalies (Fig. 6d; $Eu/Eu^* = 0.77–0.90$). These basic rocks show trace element patterns that are consistent with those of ocean island basalts (OIB) (Fig. 7d). Nb/La (0.68–0.91) and Zr/Nb (6.12–8.88) ratios are also similar to those of OIB, suggesting that they might be derived from the asthenosphere. Their low Rb/Sr and Sm/Nd ratios (0.02–0.13 and 0.19–0.22, respectively), initial ($^{87}Sr/^{86}Sr$) ratios (between 0.705 and 0.707, except sample GZ-38) and low $^{143}Nd/^{144}Nd$ ratios (between 0.51231 and 0.51237) are similar to those of the ocean island basalts in Walvis Ridge (Saunders and Tarney, 1988). The ε_{Nd} (T) values of these alkaline basic rocks (−0.47 to +0.80 for diabases, and +0.93 to +2.69 for basalts) also indicate that they might have not derived from the very depleted mantle source.

5.5. Breccia basalts from Gaoqiao of Xinhua

Breccia basalts from Gaoqiao of Xinhua are tholeiitic, with high TiO_2, low Na_2O, Fe_2O_3/FeO ratios close to 1.0, and CaO/Na_2O ratios over 4.8. Their LREE, especially the MREE, are enriched relative to the HREE [Fig. 6e; $(La/Yb)_N = 14.09–14.71$; $(Gd/Yb)_N = 6.99–7.00$]. The primitive mantle-normalized patterns of trace element exhibit a “dome” shape, with a clear Ti depletion and slight Nb and Y depletions (Fig. 7e), which are distinct from typical island-arc basalts. The abundances of trace elements, especially LREE, MREE, Zr and Hf, are similar to those of OIB, suggesting that their mantle source should also be enriched.

5.6. Granites from northeastern Hunan

Granites from northeastern Hunan are strongly peraluminous granites. They have moderate SiO_2 (68.26–72.72 wt%) and relatively high ($TiO_2 + FeO^t + MgO$) values (3.90–7.73 wt%), with $Na_2O + K_2O$ (5.95–7.32 wt%), K_2O/Na_2O (∼1.59), CaO/Na_2O (>0.3) and Rb/Sr ratios (1.52–4.25) resembling typical S-type granites in the Lachlan Fold Belt, SE Australia (Chappell and White, 2001). The REE patterns show an evident LREE and MREE enrichment relative to HREE (average $(La/Yb)_N$ values of 8.66 and $(Gd/Yb)_N$ values of 1.80) with moderate Eu negative anomalies (Fig. 6f; $Eu/Eu^* = 0.39–0.60$). Sample DW-33-1 shows elevated HREE patterns (Fig. 6f) due to the presence of garnet. These granites exhibit an enrichment of LILE (such as Th, etc.) relative to HFSE (Fig. 7f; such as Nb and Ti, etc.), which are typical features of subduction-related components, similar to the granites of Xiuning and Xucun plutons in the eastern part of the Jiangnan orogen (Xu and Zhou, 1992). The initial ($^{87}Sr/^{86}Sr$) ratios are very low (0.688–0.710), suggesting that their Rb–Sr isotopic system might be disturbed by the late tectono-thermal events which may lead to radiogenic Sr loss (Samson et al., 1995). The initial ($^{87}Sr/^{86}Sr$) ratio of sample CS-30 is even lower than 0.700 for their relative high Rb/Sr ratio. Average ε_{Nd} (T) of these granites is −2.34, in line

with the Neoproterozoic strongly peraluminous granites in Xiuning and Xucun (Xu, 1989; Li et al., 2003a).

6. Tectonic setting and petrogenesis

6.1. Basalts from Nanqiao

The highly depleted basalts from Nanqiao are within or close to the N-MORB field in the 2Nb–Zr/4-Y, Ti/Y versus Nb/Y, Ti versus Zr and $(Tb/Ta)_N$ versus $(Th/Ta)_N$ tectonic discriminative diagrams, as shown in Fig. 8. These N-MORB basalts may represent the fragments of old oceanic crust. The location of Nanqiao is far from the "Xiushui-Maoyuan back-arc basin" in the north of "Jiuling old arc" (Shu et al., 1995), but near the E-W trending "Wanzai-Nanchang" subduction zone distributed along the southern margin of the Jiuling old arc (Fig. 1). Therefore, it is possible that the Nanqiao basalts with N-MORB features are not the back-arc basin basalts, but represent the fragments of an "upper oceanic crust" locally obducted along the subduction zone. It may also represent the relicts of oceanic crust

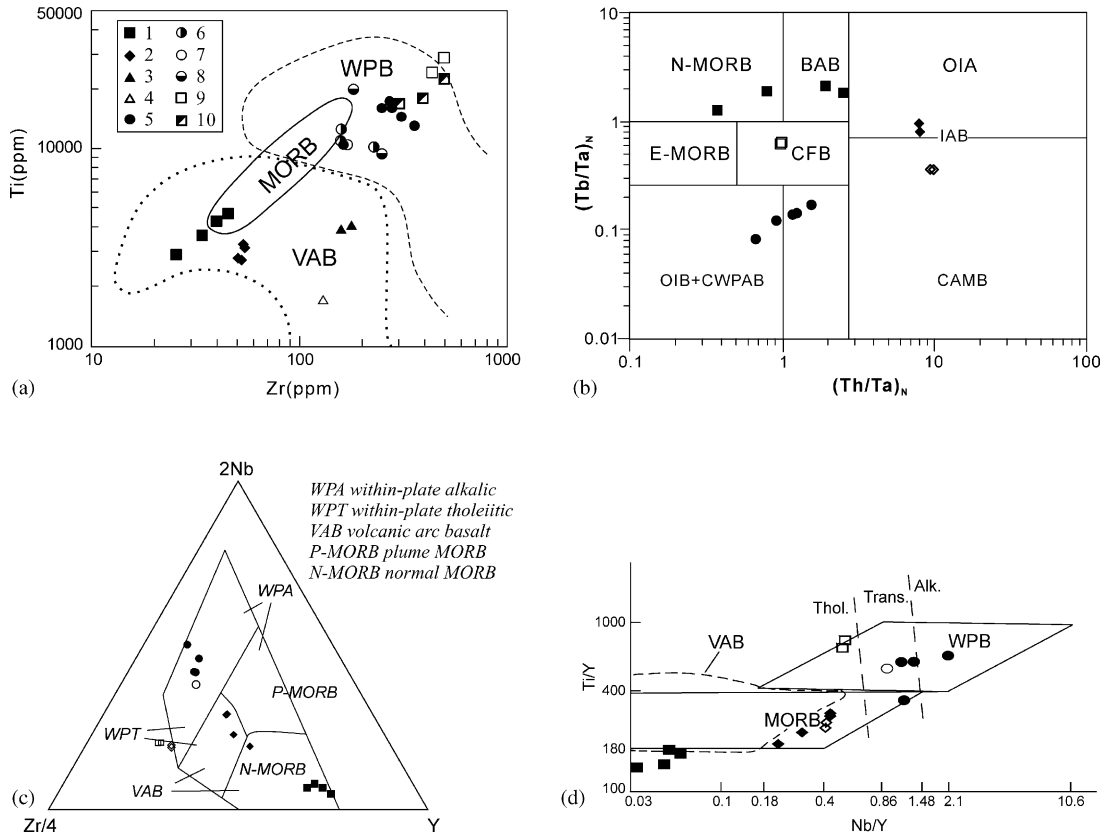

Fig. 8. Tectonic discriminative diagrams for the Meso- to Neoproterozoic basic rocks from Hunan Province. (a) Ti–Zr plot (after Pearce, 1982). *Note*: (1) Basalts from Nanqiao; (2) komatiitic basalts from Yiyang; (3)–(4) andesitic agglomerates and breccias from Baolinchong of Yiyang; (5)–(6) basic rocks from Qianyang; (7)–(8) basic rocks from Guzhang; (9)–(10) breccia basalts from Gaoqiao. (1–3, 5, 7 and 9) this study, (4) data from Jin et al. (1998), (6) data from He (1995), (8) data from Liu et al. (1993), (10) data from Chen et al. (1998). (b) $(Tb/Ta)_N$–$(Th/Ta)_N$ diagram (after Fekkak et al., 2001). *Note*: N-MORB: "normal" MORB, E-MORB: enriched MORB, BAB: back-arc basin basalts, CFB: continental flood basalts, OIA: Mariana-type intra-oceanic arc, IAB: intermediate arc basalts, OIB: ocean island basalts, CWPAB: continental within-plate alkali and transitional basalts; and CAMB: active continental margin basalts. Symbols as in Fig. 2. (c) 2Nb–Zr/4-Y diagram (after Meschede, 1986). *Note*: Symbols as in Fig. 2. (d) Ti/Y–Nb/Y diagram (after Pearce, 1982). *Note*: Symbols as in Fig. 2. VAB: volcanic arc basalt; WPB: within-plate basalt; MORB: mid-ocean ridge basalt; Thol., tholeiitic; Trans., transitional; Alk., alkaline.

in a "forearc basin". The geological fact that the basic rocks with N-MORB characters occur near the subduction zone provides new evidence for the existence of the Mesoproterozoic "Jiuling old arc" (Zhou et al., 2003).

6.2. Komatiitic basalts from Yiyang

The Mesoproterozoic Komatiitic basalts from Yiyang are shown in the volcanic arc basalt field on the Ti versus Zr diagram (Fig. 8a) and in the island-arc basalts field on the $(Tb/Ta)_N$ versus $(Th/Ta)_N$ diagram (Fig. 8b). Their geochemical features are similar to those of the komatiitic basalts in the Vetreny belt (southeastern Baltic Shield) whose arc-magma characteristics were regarded as results of crustal contamination (Puchtel et al., 1996). However, the komatiitic basalts from Yiyang, with the geochemical features of both arc and plume magmas, do not show any positive correlation between $(Nb/Th)_N$ and ε_{Nd}, or the negative correlations of $(La/Sm)_N$ versus ε_{Nd}, $(La/Sm)_N$ versus $(Nb/Th)_N$ and Zr/Y versus $(Nb/Th)_N$ due to crustal contamination (Puchtel et al., 1996). Therefore, the geochemistry of the komatiitic basalts from Yiyang may reflect the inherited signatures from their magma sources.

In the late Archaean Abitibi greenstone belts, Canada, almost coeval (2.7 Ga) arc-type tholeiites and calc-alkaline volcanics are associated with plume-derived komatiites. Contemporaneous subduction and plume magmatism did occur in Abitibi greenstone belts. These assemblages have been regarded as evidence of interaction between the arcs and plumes (Wyman, 1999; Wyman et al., 2002). The close spatial and temporal associations of both arcs and plumes were also reported in the Cretaceous Caribbean magmatism (White et al., 1999). In the Tonga arc, the komatiitic lava derived from the Samoan plume could flow in the early arc setting (Farley, 1995). Thus, it is seen that arc and plume magmatism may not be exclusive but, sometimes, correlated with each other. On the basis of the model presented by Wyman (1999), arc volcanism may occur before, during and after plume activity. The interactions between arc and plume were probably caused by subduction step back at the margin of hotspot (Wyman, 1999) or the subduction of plume-modified spreading centers (Hollings and Wyman, 1999). It should be pointed that the plumes of Wyman (1999) are different in geological context from those of Li et al. (1999). The former are small-scale, local and directly related to plate tectonics, whereas the latter are large-scale and not directly related to plate tectonics. The komatiitic basalts from Yiyang are companied with arc tholeiites (Xiao, 1983; HRGST, 1988; He and Han, 1992). We have no enough geological or petrological evidence to argue whether subduction step back or the subduction of spreading center was responsible for the association of plume-derived komatiitic basalts and arc-type volcanic-intrusive rocks in the Lengjiaxi Group of Yiyang. However, the occurrence of the komatiitic basalts in an arc-type assemblage in the Lengjiaxi Group of this area suggests that the local interaction between an arc and a plume during the Mesoproterozoic did exist along southern margin of the Yangtze block (Zhou et al., 2004). Thus, it is evident that the geochemical features of arc basalt for the komatiitic basalts from Yiyang might be caused by local complex interaction between the arc and the plume, rather than the results of crustal contaminations.

6.3. Andesitic agglomerates and breccias from Baolinchong

Neoproterozoic andesitic agglomerates and breccias from Baolinchong of Yiyang are plotted close to within-plate tholeiite (WPT) area on 2Nb–Zr/4-Y diagram (Fig. 8c). However, they belong to volcanic arc basalt area on the Ti versus Zr diagram (Fig. 8a), and are close to the same area on the Ti/Y–Nb/Y diagram (Fig. 8d). Furthermore, they are in active continental margin basalt (CAMB) field on the $(Tb/Ta)_N$ versus $(Th/Ta)_N$ diagram (Fig. 8b). All of them suggesting an island-arc setting. Both LILE enrichments and Nb and Ti negative anomalies also imply their arc magma characters.

6.4. Basic rocks from Qianyang, Guzhang and Gaoqiao

The Neoproterozoic basalts and diabases from Qianyang and Guzhang straddle the boundary between OIB and CWPAB on the $(Tb/Ta)_N$ versus $(Th/Ta)_N$ diagram (Fig. 8b), but fall in the within-plate basalt (WPB) field on 2Nb–Zr/4-Y, Ti/Y–Nb/Y and Ti–Zr diagrams (Fig. 8a, c and d). These alkali basalts, with primitive mantle-normalized patterns of LILE similar to OIB,

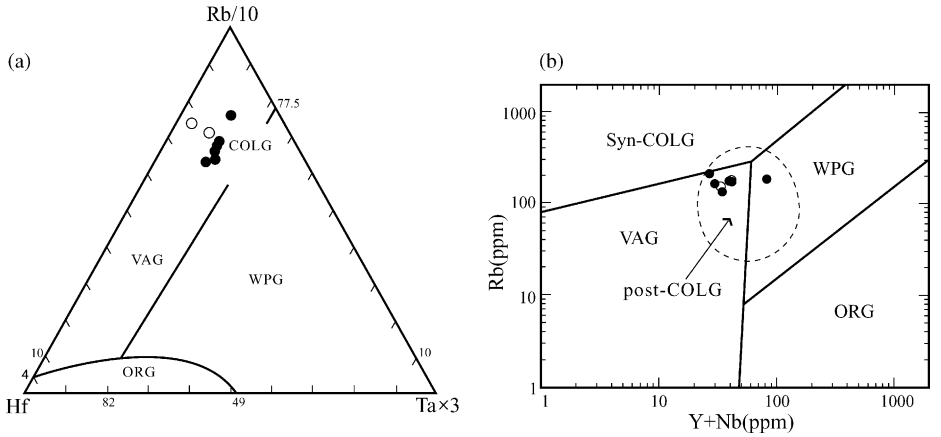

Fig. 9. Tectonic discriminative diagrams for the Neoproterozoic granites from northeast Hunan. (a) Rb/10-Hf–Ta × 3 plot (after Harris et al., 1986); (b) (Y + Nb)–Rb plot (after Pearce et al., 1984) with field for post-collision granites (post-COLG) from Pearce (1996). Solid circle, this study; open circle, data from Wu et al. (2001).

might be formed in continental rifts or in oceanic islands settings.

The Sinian breccia basalts from Gaoqiao of Xinhua belong to the CFB field on the $(Tb/Ta)_N$ versus $(Th/Ta)_N$ diagram (Fig. 8b), but fall in or close to the WPB field on the other three tectonic discriminative diagrams (Fig. 8a, c and d). They occur in the Sinian rifting basin. It is doubtless that they are the typical rifting basalts (Chen et al., 1998). Thus, their formation, corresponding to the diabases and basalts from Qianyang and Guzhang, might be correlated with the Neoproterozoic rifting event in South China.

6.5. Granites from northeastern Hunan

The strongly peraluminous granites from northeastern Hunan fall within the collision granite field in the Rb/10-Hf–Ta × 3 diagram (Fig. 9a), and they are also located in the field of post-collisional granite on (Y + Nb) versus Rb diagram (Fig. 9b), suggesting that the SP granitic magmas were generated during the post-collisional stage (Liegeois, 1998). Sample DW-33-1 is located in the WPG (within-plate granite) area in Fig. 9b, due to its high Y contents resulted from appreciable garnets in it, which is confirmed by its high HREE (Fig. 6f). Source rocks for the SP granites from NE Hunan Province should be psammitic for their high CaO/Na_2O (>0.3) and magmatogenic cordierite minerals (Sylvester, 1998). Their Nd model ages range from 1634 to 1707 Ma (Table 2), which are comparable with those of the Mesoproterozoic sedimentary rocks from the southern margin of Yangtze Block (Li et al., 1991; Chen and Jahn, 1998). This implies that the Mesoproterozoic strata may be the sources for the SP granitic magma. On the other hand, the metamorphic sedimentary rocks of the Mesoproterozoic Lengjiaxi Group in northeastern Hunan Province are dominantly psammitic to pelitic in composition (Xiao et al., 2002). Thus, it is believed that these SP granitic magmas should be the products of the partial melting of the psammitic rocks in the Mesoproterozoic Lengjiaxi Group.

7. Implications for the tectono-magmatic evolution

The Jiangnan orogen was previously considered to be the products of late Meso- to early Neoproterozoic orogenic events (Guo et al., 1984; Shui, 1987; Xing et al., 1992; Zhou and Zhu, 1993; Li and Mu, 1999), which led Li et al. (1995, 1999) to correlate it with the Grenville-aged orogens, and to propose that the South China was an important part of Rodinia. However, recent isotopic dating indicates that the collisional event between the Yangtze and Cathysia blocks took place during Neoproterozoic (ca. 870–820 Ma) rather than Grenvillian (ca. 1100–900 Ma). The high-pressure glaucophane-bearing schists from Huaiyushan of

Jiangxi Province, the central part of Jiangnan orogen, gave a K–Ar age of 866 ± 14 Ma (Shu et al., 1993). Amphibole from the blueschists from NE Jiangxi Province yielded an Ar–Ar age of ca. 857.4 ± 18.3 Ma (Xu et al., 1992). A similar high-pressure metamorphic event has also been reported from the Mayuan Group from the northern part of Fujian Province in the Cathaysia (Zhao and Cawood, 1999). New zircon SHRIMP U–Pb date shows that the S-type granites distributed along the Jiangnan orogen were emplaced at ∼820 Ma (Li, 1999; Li et al., 2003a). In fact, the 870–820 Ma orogenic event is not unique to South China; it has also been reported from northeastern Zimbabwe (Vinyu et al., 1999) and Yenisei fold belt (Safonov, 1997). The Grenvillian continental collision in South China was first proposed by Li et al. (2002b) who, however, did not provide reliable metamorphic ages. Recently, the ∼825 Ma mafic–ultramafic rocks and granitic rocks distributed along the Jiangnan orogen have been regarded as the results of the upwelling of a superplume which led to the breakup of the Rodinia supercontinent (Li et al., 2002a, 2003a, 2003b, 1995). On the other hand, the superplume model is questioned by regional geology, petrology and geochronology (Zhou et al., 2002, 2004; Wang et al., 2004). P–T–t studies of the Mayuan assemblage in the Cathaysia also suggested a mid-Neoproterozoic collisional rather than an intra-cratonic events (Zhao and Cawood, 1999). Detailed geochronological and geochemical studies of the Meso- to Neoproterozoic basic–acid rocks will provide insights into the history of the Precambrian tectono-magmatism of the orogen in the area.

7.1. Subduction of the Mesoproterozoic oceanic crust

The occurrence of the Mesoproterozoic typical N-MORB from Nanqiao of Liuyang near the subduction zone, combined with the island-arc features of the komatiitic basalts occurring in the Lengjiaxi Group in Yiyang, indicates that oceanic subduction and arc activities existed in the HPWJO during the Mesoproterozoic, as in the eastern part of the Jiangnan orogen and other areas in its western part (Guo et al., 1984; Zhou and Zhu, 1993; Xing et al., 1992). These may represent the prelude of the early Jinningian orogeny in the area (Fig. 10a). At ca. 870 Ma, the subduction may have been completed, and the collision between the Yangtze and Cathysia blocks took place, which finally led to the formation of the Jiangnan orogen, NEE stretching over 1500 km long. The Mesoproterozoic Lengjiaxi Group with a NE-NEE trending fold axis experienced extensive low-grade metamorphism. There is an obvious unconformity between the Lengjiaxi Group and the Banxi Group in the area, which is considered as important geological evidence for the Jinningian orogeny.

7.2. Slab breakoff during the Mid-Neoproterozoic

The SP granites from northeastern Hunan have been traditionally regarded as the products of the syn-collisional magma activities during the orogeny (Xu, 1989; Luo, 1994). Recently, however, it has been proposed that the formations of the Neoproterozoic SP granites along the Jiangnan orogen might be triggered by a ∼825 Ma superplume beneath South China (Li et al., 2003a). We think it is most likely that the SP granites are the products of post-collisional magmatism, and their origin may have been related to the breakoff of the subducted oceanic slab. The major evidence is summarized as follows:

(1) The ca. 870 Ma high-pressure glaucophane-bearing schists from Huaiyushan of Jiangxi Province (the central part of Jiangnan orogen) represent the peak of the Neoproterozoic collision event between the Cathaysia and the Yangtze Block. They are older than the ca. 819 Ma Neoproterozoic peraluminous granites from NE Hunan and NW Jiangxi. Moreover, it was observed in the field that the foliation of the blueschists in NE Jiangxi is cut locally by the regional schistosity, which is in turn cross-cut by the SP granites (Charvet et al., 1996). Thus, the SP granites should have been emplaced during the post-collisional stage.
(2) Geochronological and geochemical characteristics of the SP granites from northeastern Hunan are similar to those of the granites in Xiuning, Shexian and Xucun plutons in the eastern Jiangnan orogen and the Sanfang pluton in the western Jiangnan orogen (Li, 1999; Li et al., 2003a). Their zonal distribution along the NEE trending Jiangnan orogen indicates that the formations of these SP granites may not be correlated with the mantle plume.

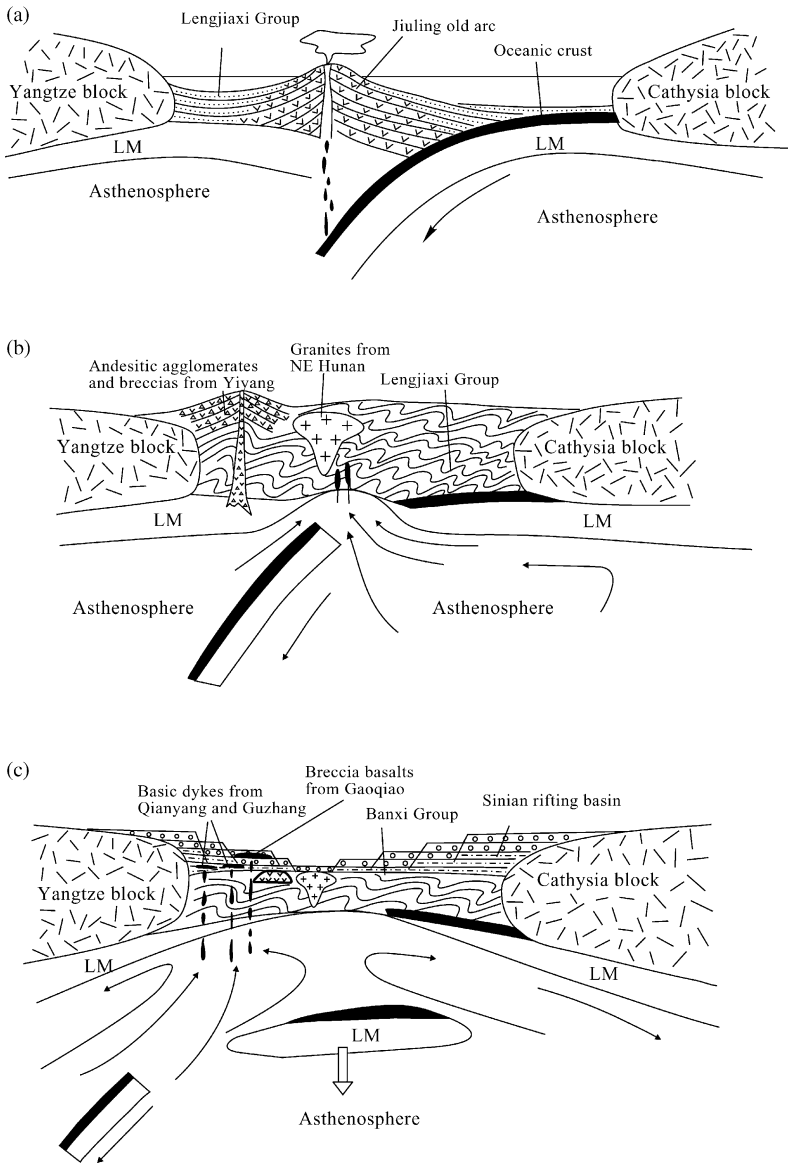

Fig. 10. Sketch evolution model for western Jiangnan orogen in Hunan Province during Meso- to Neoproterozoic. (a) ~1300 Ma, (b) 870–820 Ma and (c) 820–680 Ma.

(3) It has been generally accepted that a large number of S-type granites in orogens emplaced during the post-collisional stage (Liegeois, 1998; Sylvester, 1998). Davies and Blanckenburg (1995) proposed that the breakoff of a subducted lithospheric slab is a natural consequence of an ocean closure. For example, the slab breakoff occurred after subduction and collision in both the Alps and northwest Himalayas orogens (O'brien, 2001). It was reported that the basic rocks and/or k-rich lamprophyres, in general, are accompanied with a slab breakoff (Davies and Blanckenburg, 1995; Atherton and Ghani, 2002). It has also been found that there are a few spessartites dykes intruded the Lengjiaxi

Group about 5 km north of the SP granite intrusions in northeastern Hunan. In addition, many basic rocks intruded the Lengjiaxi Group have been found along the southeastern margin of the eastern Jiuling granite intrusion in Jiangxi Province. The occurrences of these spessartites and basic rocks may provide further evidence for the possible slab breakoff event.

The andesitic rocks from Baolinchong, coeval with the SP granites from NE Hunan, have also been formed after the peak collision, suggesting that they are also the products of the post-collisional magmatisms. Andesites generated from the post-collisional settings in the world have also been reported by Zeck et al. (1998).

Taken together, the model of subducted slab breakoff can well explain the genesis of the Neoproterozoic SP granites and andesitic rocks in the HPWJO. A geological evolutionary model for the HPWJO between 870 and 820 Ma is simply described in Fig. 10b. First, the north-toward subduction of the oceanic crust in the north of the Cathysia Block continued during the early Neoproterozoic. Then, the slab breakoff occurred after the peak collision between the Cathysia and Yangtze blocks. This led to the eruption of the andesitic magma and to the underplating of the deeper asthenosphere magma, causing a large scale partial melting of the metamorphic rocks of the Lengjiaxi Group to form granitic magma in the middle to lower crust. The latter, then, ascended and captured fragments of the wall rocks, and finally emplaced in the middle to shallow crustal level.

7.3. Rifting in the HPWJO

A superplume model was put forward by Li et al. (1999, 2003b) to explain the ~825 Ma mafic-ultramafic rocks and coeval granites in northern Guangxi, South China. However, were the formations of these Neoproterozoic basic–acid rocks related to a superplume? Where was the Proterozoic superplume? These questions bring about a hot debate. Magmatism related to a superplume event in northern Guangxi as proposed by Li et al. (1999, 2003b) was questioned by Zhou et al. (2004), who found no rifting magmatism in the western Jiangnan orogen ~820 Ma ago. The 760–750 Ma basic rocks from western Hunan and the 750–680 Ma Sinian breccia basalts from central Hunan, with typical geochemical features of OIB, may represent a rifting event in the area. This, however, is most probably induced by the breakoff of a subducted lithospheric slab during the post-collision, rather than a plume event.

Fig 10c shows a preliminary model for the formation and evolution of the basic magmas in the HPWJO during late Neoproterozoic. The breakoff of the subducted slab led to the extension of the lithosphere under the southern margin of the Yangtze block. Then, the underplating and ascending of the asthenosphere-derived magma caused the eruption of within-plate basic magmas having OIB characteristics, which might represent the beginning of the rifting in HPWJO. Finally, the occurrence of the breccia basalts from the Sinian basin (Chen et al., 1998), may indicate the continuous rifting along the southeastern margin of the Yangtze block. Both the distribution style and field evidence of these basic rocks do not accommodate a mantle plume model. Therefore, our conclusion is that geological events related to the rifting in the HPWJO may have resulted from the post-collisional extension, breakoff of a subducted slab and collapse of the orogen rather than the uprising of a superplume as proposed by Li et al. (1999, 2003b).

8. Conclusions

The Meso- to Neoproterozoic basic–acid rocks located in HPWJO may record the evolution of the western Jiangnan orogen in South China. The Mesoproterozoic basic rocks with arc signatures are the products of stage-different magmatism of the Jinningian orogeny, which finally led to the formation of the Jiangnan orogen at 870–820 Ma. The Jiangnan orogen is different in age from the Grenvillian orogen, which is considered to have led to the assembly of Rodinia. The Neoproterozoic granites from northeastern Hunan and the andesitic rocks from Baolinchong in central Hunan are the products of post-collisional magmatisms related to the subducted slab breakoff, not related to superplume activities. The Neoproterozoic basic rocks with OIB-like geochemical features from western Hunan may be considered to represent the beginning of the rifting in the HPWJO. The Sinian breccia basalts from Gaoqiao of central Hunan suggest a continuous rifting process. The rifting in the HPWJO is considered to have resulted from the post-collisional extension, breakoff

of a subducted slab and collapse of the orogen, rather than a superplume event.

Acknowledgements

This research was financially supported by the National Natural Science Foundation of China (grants No. 49872030 and No. 40221301), Postgraduate Training Project of Jiangsu Province, China, and the State Key Laboratory for Mineral Deposit Research, Nanjing University, China. Prof. L. Liu (Inst. Earth Sciences, Academia Sinica, Taiwan) and Dr. S.Z. Chen (Geomatrix Consultants Inc., USA) are thanked for their constructive comments and grammatical corrections on the manuscript. We also thank Prof. X.M. Zhou (Nanjing University, China) for advice of the earlier version of the manuscript, J.Z. Huang, X.S. Tang for their earnest direction and assistance on the field trip, J.P. Xu, M.Q. Zhang and D. Liu for major element analysis, L.W. Qiu for trace element analysis, R.H. Zhang and J. Qiu for Sr–Nd isotopic analysis. Special thanks are expressed to Guochun Zhao and an anonymous reviewer for their critical and constructive comments that led to substantial changes and improvements in this manuscript.

References

Atherton, M.P., Ghani, A.A., 2002. Slab breakoff: a model for Caledonia, Late Granite syn-collisional magmatism in the orthotectonic (metamorphic) zone of Scotland and Donegal. Ireland Lithos 62, 65–85.

BGMRHP (Bureau of Geology and Mineral Resources of Hunan Province), 1988. Regional Geology of Hunan Province. Geological Publishing House, Beijing (in Chinese, with English Abstract).

Chappell, B.W., White, A.J.R., 2001. Two contrasting granite types: 25 years later. Aust. J. Earth Sci. 48, 489–499.

Charvet, J., Shu, L.S., Shi, Y.S., Guo, L.Z., Faure, M., 1996. The building of South China: collision of Yangtze and Cathaysia blocks, problems and tentative answers. J. Southeast Asian Earth Sci. 13, 223–235.

Chen, D.F., Pan, J.M., Xu, W.X., Chen, G.Q., Chen, X.P., 1998. Geochemistry of Sinian basalts from South China and its Tectonic Setting. Acta Pertrologica Sinica 14, 343–350 (in Chinese, with English Abstract).

Chen, J.F., Foland, K.A., Xing, F.M., Xu, X., Zhou, T.X., 1991. Magmatism along the southeast margin of the Yangtze block: Precambrian collision of the Yangtze and Cathysia blocks of China. Geology 19, 815–818.

Chen, J.F., Jahn, B.M., 1998. Crustal evolution of southeastern China: evidence from Sr, Nd and Pb isotopic compositions of granitioids and sedimentary rocks. Tectonophysics 284, 101–133.

Condie, K.C., 1989. Geochemical changes in basalts and andesites across the Archean-Proterozoic boundary: identification and significance. Lithos 23, 1–18.

Davies, J.H., Blanckenburg, F.V., 1995. Slab breakoff: a model of lithosphere detachment and its test in the magmatism and deformation of collisional orogens. Earth Planet. Sci. Lett. 129, 85–102.

Farley, K.A., 1995. Rapid recycling of subducted sediments into the Samoan mantle plume. Geology 23, 531–534.

Fekkak, A., Pouclet, A., Ouguir, H., Ouazzani, H., Badra, L., Gasquet, D., 2001. Geochemistry and geotectonic significance of Early Cryogenian volcanics of Saghro (Eastern Anti-Atlas, Morocco). Geodinamica Acta 14, 373–385.

Franzini, M., Leoni, L., Saitta, M., 1972. A simple method to valuate the matrix effect in X-ray fluorescence analysis. X-ray Spectrom. 1, 151–154.

Guo, L.Z., Shi, Y.S., Ma, R.S., 1980. The geotectonic framework and crustal evolution of South China. In: Scicentific Paper on Geology for International Exchange. J. Geological Publishing House, Beijing (in Chinese, with English Abstract).

Guo, L.Z., Yu, J.H., Shi, Y.S., Ma, R.S., Lu, H.F., Yun, L.L., Zhu, H.J., Yang, S.F., Chen, S.Z., 1984. On the time and space distribution of the granitic rocks and their relations to the tectonic configuration and crustal evolution in the southeastern China. In: Xu, K., Tu, G. (Eds.), Geology of Granites and Their Metallogenetic Relations. Science and Technology Press, Nanjing, Jiangsu, pp. 38–48 (in Chinese, with English Abstract).

Haack, U., 1983. On the content and vertical distribution of K, Th and U in the continental crust. Earth Planet. Sci. Lett. 62, 360–366.

Harris, N.B.W., Pearce, J.A., Tindle, A.G., 1986. Geochemical characteristics of collision-zone magmatism. In: Coward, M.P., Ries, A.C. (Eds.), Collision Tectonics, vol. 19. Geol. Soc. Spec. Publ., pp. 67–81.

He, A.S., Han, X.G., 1992. Characteristics and geological environment of volcanic rocks from Yiyang. Hunan Geol. 11, 269–274 (in Chinese, with English Abstract).

He, A.S., 1995. Geochemistry of basic-ultrabasic rocks from Aikou area in the west of Hunan Province. Geotectonica Metallogenia 19, 239–247 (in Chinese, with English Abstract).

Hollings, P., Wyman, D., 1999. Trace element and Sm–Nd systematics of volcanic and intrusive rocks from the 3 Ga Lumby Lake Greenstone belt: Superior Province: evidence for Archean plume–arc interaction. Lithos 46, 189–213.

Hollings, P., Wyman, D., Kerrich, R., 1999. Komatiite-basalt-rhyolite volcanic associations in Northern Superior Province greenstone belts: significance of plume–arc interaction in the generation of the proto continental Superior Province. Lithos 46, 137–161.

HRGST (Hunan Regional Geological Survey Team), 1976. Regional Geological Survey Report (Liuyang area, 1:200000) (in Chinese).

HRGST (Hunan Regional Geological Survey Team), 1988. Regional Geological Survey Report (Yiyang area, 1:50000) (in Chinese).

Hsü, K., Sun, S., Li, J., Chen, H., Pen, H., Sengor, A., 1988. Mesozoic overthrust tectonics in South China. Geology 16, 418–421.

Huang, X.L., Wang, L.C., Chen, X.M., Hu, H., Liu, C.S., 2002. Vertical variation in the mineralogy of the Yichun topaz-lepidolite granite, Jiangxi Province, southern China. Can. Mineral. 40, 1047–1068.

Jin, H.S., Fu, L.W., 1986. The evolution of volcanic rocks in Hunan Province and their implications in plate tectonics. Geol. Rev. 32, 225–235 (in Chinese, with English Abstract).

Jin, W.S., Zhao, F.Q., Wang, Z.W., Gan, X.C., 1998. Geochemistry of Meso-Proterozoic rocks from Xiangdongbei-Guibei. Guangxi Geol. 11, 60–64 (in Chinese, with English Abstract).

Li, X.H., Zhao, Z.H., Gui, X.T., Yu, J.S., 1991. Sm–Nd isotopic and zircon U–Pb constraints on the age of formation of the Precambrian crust in southeast China. Geochimica 3, 255–264 (in Chinese, with English Abstract).

Li, Z.X., Zhang, L.H., Powell, C.M., 1995. South China in Rodinia: a part of the missing link between Australia-east Antarctica and Laurentia? Geology 23, 407–410.

Li, X.H., Zhao, J.X., McCulloch, M.T., Zhou, G.Q., Xing, F.M., 1997. Geochemical and Sm–Nd isotopic study of Neoproterozoic ophiolites from southeastern China: petrogenesis and tectonic implications. Precam. Res. 81, 129–144.

Li, J.H., Mu, J., 1999. Tectonic constraints from Chinese cratonic blocks for the reconstruction of Rodinia. Sci. Geol. Sinica 34, 259–272 (in Chinese, with English Abstract).

Li, X.H., 1999. U–Pb zircon ages of granites from the southern margin of the Yangtze margin: timing of Neoproterozoic Jinning: orogen in SE China and implication for Rodinia assembly. Precam. Res. 97, 43–57.

Li, Z.X., Li, X.H., Kinny, P.D., Wang, J., 1999. The breakup of Rodinia: did it start with a mantle plume beneath South China? Earth Planet. Sci. Lett. 173, 171–181.

Li, X.H., Li, Z.X., Zhou, H.W., Liu, Y., Kinny, P.D., 2002a. U–Pb zircon geochronology, geochemistry and Nd isotopic study of Neoproterozoic bimodal volcanic rocks in the Kangdian Rift of South China: implications for the initial rifting of Rodinia. Precam. Res. 113, 135–154.

Li, Z.X., Li, X.H., Zhou, H.W., Kinny, P.D., 2002b. Grenvillian continental collision in South China: new SHRIMP U–Pb zircon results and implications for the configuration of Rodinia. Geology 30, 163–166.

Li, X.H., Li, Z.X., Ge, W.C., Zhou, H.W., Li, W.X., Liu, Y., Wingate, M.T.D., 2003a. Neoproterozoic granitoids in South China: crustal melting above a mantle plume at ca. 825 Ma? Precam. Res. 122, 45–83.

Li, Z.X., Li, X.H., Kinny, P.D., Wang, J., Zhang, S., Zhou, H.W., 2003b. Geochronology of Neoproterozoic syn-rift magmatism in the Yangtze Craton, South China and correlations with other continents: evidence for a mantle superplume that broke up Rodinia. Precam. Res. 122, 85–109.

Liegeois, J.P., 1998. Some words on the post-collisional magmatism. Lithos 45, XV–XVII.

Liu, C.S., Ling, H.F., Xiong, X.L., Shen, W.Z., Wang, D.Z., Huang, X.L., Wang, R.C., 1999. An F-rich Sn-bearing volcanic-intrusive complex in Yanbei, South China. Econ. Geol. 94, 325–342.

Liu, H.C., Zhu, B.Q., 1994. Geochronology study of Banxi Group and Lengjiaxi Group from Western Hunan Province. Chin. Sci. Bull. 39, 148–150 (in Chinese, with English Abstract).

Liu, J.S., He, S.X., Xiao, X.D., 1993. Geochemistry and geotectonic setting of Wanyan volcanic-intrusive complex in Hunan, South China. J. Cent.-South Inst. Min. Met. 24, 149–155 (in Chinese, with English Abstract).

Liu, Z.W., 1994. Geochemistry of Precambrian volcanic rocks in Hunan and their tectonic setting. Hunan Geol. 13, 137–146 (in Chinese, with English Abstract).

Lu, S.N., 2001. From Rodinia to Gondwanaland supercontinents-thinking about problems of researching Neoproterozoic supercontinents. Earth Sci. Front. 8, 441–448 (in Chinese, with English Abstract).

Luo, H.Y., 1994. "Baolinchong Formation" and the necessity of its establishment. Hunan Geol. 13, 72–74 (in Chinese, with English Abstract).

Maitre, R.W.L., Bateman, P., Dudek, A., Keller, J., Lemeyre, J., Bas, M.J.L., Sabine, P.A., Schmid, R., Sorensen, H., Streckeisen, A., Wooley, A.R., Zanettin, B., 1989. A Classification of Igneous Rocks and Glossary of Terms. Blackwell, Oxford.

Maniar, P.D., Piccolli, P.M., 1989. Tectonic discrimination of granitoid. Geol. Soc. Am. Bull. 101, 635–643.

Mattioli, M., Guerrera, F., Tramontana, M., Raffaelli, G., D'Atri, M., 2000. High-Mg tertiary basalts in Southern Sardinia (Italy). Earth Planet. Sci. Lett. 179, 1–7.

Meschede, M., 1986. A method of discriminating between different types of mid-ocean ridge basalts and continental tholeiites with the Nb–Zr–Y diagram. Chem. Geol. 56, 207–218.

Nisbet, E.G., Cheadle, M.J., Arndt, N.T., Bickle, M.J., 1993. Constraining the potential temperature of the Archean mantle: a review of the evidence from komatiites. Lithos 30, 291–307.

O'brien, P.J., 2001. Subduction by collision: Alpine and Himalayan examples. Phys. Earth Planet. Interiors 127, 277–291.

Pang, Y.K., 1983. Geological characteristics of Xuefengian granites from Hunan Province. Hunan Geol. 2, 22–30 (in Chinese).

Pearce, J.A., 1982. Trace element characteristic of lavas from destructive plate boundaries. In: Thorpe, R.S. (Ed.), Andesites. Wiley, New York, pp. 528–548.

Pearce, J.A., 1996. Sources and settings of granitic rocks. Episodes 19, 120–125.

Pearce, J.A., Harris, N.B.W., Tindle, A.G., 1984. Trace element discrimination diagrams for the tectonic interpretation of granitic rocks. J. Petrol. 25, 956–983.

Puchtel, I.S., Haase, K.M., Hofmann, A.W., Chauvel, C., Kulikov, V.S., Garbe-Schonberg, C.D., Nemchin, A.A., 1996. Petrology and geochemistry of crustally contaminated komatiitic basalts from the Vetreny Belt, southeastern Baltic Shield: evidence for an early Proterozoic mantle plume beneath rifted Archean continental lithosphere. Geochim. Cosmochim. Acta 61, 1205–1222.

Safonov, Y.G., 1997. Hydrothermal gold deposites-distribution, geological/genetic types, and productivity of ore-forming systems. Geol. Ore Deposits 39 (1), 20–32.

Samson, S.D., Coler, D.G., Speer, J.A., 1995. Geochemical and Nd–Sr–Pb isotopic composition of Alleghanian granites of the southern Appalachians: origin, tectonic setting, and source characterization. Earth Planet. Sci. Lett. 134, 359–376.

Saunders, A.D., Tarney, J., 1988. Origin of MORB and chemically depleted mantle reservoirs: trace element constraints. J. Petrol. 425–445 (Special Lithosphere Issue).

Sensarma, S., Palme, H., Mukhopadhyay, D., 2002. Crust–mantle interaction in the genesis of siliceous high magnesian basalts: evidence from the Early Proterozoic Dongargarh Supergroup, Indian. Chem. Geol. 187, 21–37.

Shen, J., Zhang, Z.Q., Liu, D.Y., 1997. Sm–Nd, Rb–Sr, $^{40}Ar/^{39}Ar$, and $^{207}Pb/^{206}Pb$ age of the Douling metamorphic complex from eastern Qinling Orogenic belt. Earth Sci. J. China Univ. Geosci. 18, 248–254 (in Chinese, with English Abstract).

Shen, W.Z., Xu, S.J., Gao, J.F., Yang, Z.S., Yang, Q.W., 2002. Sm–Nd dating and Nd–Sr isotopic characteristics of the Shimian ophiolite suite, Sichuan Province. Chin. Sci. Bull. 47, 1897–1901.

Shu, L.S., Zhou, G.Q., Shi, Y.S., Yin, J., 1993. Study of high pressure metamorphic blueschist and its late Proterozoic age in the eastern Jiangnan belt. Chin. Sci. Bull. 38, 779–882 (in Chinese).

Shu, L.S., Shi, Y.S., Gou, L.Z., Charvet, J., Sun, Y. (Eds.), 1995. Plate Tectonic Evolution and the Kinematics of Collisional Orogeny in the Middle Jiangnan, Eastern China. Nanjing University Publ., 174 pp. (in Chinese, with English Abstract).

Shui, T., 1987. Tectonic framework of the southeastern China continental basement. Sci. Sinica 30, 414–422 (in Chinese, with English Abstract).

Sun, S.S., McDonough, W.F., 1989. Chemical and isotopic systematics of oceanic basalts: implications for mantle composition and processes. In: Saunders, A.D., Norry, M.J. (Eds.), Magmatism in the Ocean Basins, vol. 42. Geol. Soc. Spec. Publ., pp. 313–345.

Sylvester, P.J., 1998. Post-collisional strongly peraluminous granites. Lithos 45, 29–44.

Tang, X.S., Huang, J.Z., Guo, L.Q., 1997. Hunan Banxi Group and its tectonic environment. Hunan Geol. 16, 219–226 (in Chinese, with English Abstract).

Vinyu, M.L., Hanson, R.E., Martin, M.W., Bowring, S.A., Jelsma, H.A., Krol, M.A., Dirks, P.H.G.M., 1999. U–Pb and $^{40}Ar/^{39}Ar$ geochronological constraints on the tectonic evolution of the easternmost part of the Zambezi orogenic belt, northeastern Zimbabwe. Precam. Res. 98, 67–82.

Wang, J., Li, X.H., Duan, T.Z., Liu, D.Y., Song, B., Li, Z.W., Gao, Y.H., 2003. Zircon SHRIMP U–Pb dating for the Cangshuipu volcanic rocks and its implications for the lower boundary age of the Nanhua strata in South China. Chin. Sci. Bull. 48, 1663–1669.

Wang, X.L., Zhou, J.C., Qiu, J.S., Gao, J.F., 2004. Comment on "Neoproterozoic granitoids in South China: crustal melting above a mantle plume at ca 825 Ma?" by Xian-Hua Li et al. (PR 122, 45–83, 2003). Precam. Res. 132, 401–403.

Wang, J., Li, Z.X., 2003. History of Neoproterozoic rift basins in South China: implications for Rodinia breakup. Precam. Res. 122, 141–158.

White, R.V., Tarney, J., Kerr, A.C., Saunders, A.D., Kempton, P.D., Pringle, M.S., Klaver, G.T., 1999. Modification of an oceanic plateau, Aruba, Dutch Caribbean: implication for the generation of continental crust. Lithos 46, 43–68.

Winchester, J.A., Floyd, P.A., 1977. Geochemical discrimination of different magma series and their differentiation products. Chem. Geol. 20, 325–343.

Wu, G.Y., Chen, H.M., Jia, B.H., He, J.N., 2001. Genetic mechanism of the Changsanbei granitic inrusion in northern Hunan. Geol. Miner. Resour. South China 1, 23–35 (in Chinese, with English Abstract).

Wyman, D.A., 1999. A 2.7 Ga depleted tholeiite suite: evidence of plume–arc interaction in the Abitibi Greenstone belt. Can. Precam. Res. 97, 27–42.

Wyman, D.A., Kerrich, R., Polat, A., 2002. Assembly of Archean cratonic mantle lithosphere and crust: plume–arc interaction in the Abitibi-Wawa subduction–accretion complex. Precam. Res. 115, 37–62.

Xiao, X.D., 1983. On the basaltic komatiite and its formative environment in Yiyang, Hunan. J. Central-South Inst. Min. Metall. 38, 106–113 (in Chinese, with English Abstract).

Xiao, X.D., 1988. Spinifex was found in Mesoproterozoic komatiites of Yiyang, Hunan. Chin. Sci. Bull. 4, 286–288 (in Chinese).

Xiao, Y.J., Chen, G.H., Fu, G.G., 2002. Discussion on the tectonometallogenic background of the DaWan gold ore district, northeastern Hunan Province. Geotectonic Metallogenia 26, 143–147 (in Chinese, with English Abstract).

Xing, F.M., Xu, X., Chen, J.F., Zhou, T.X., Foland, K.A., 1992. The late Proterozoic continental accretionary history of the southeastern margin of the Yangtze platform. Acta Geologica Sinica 66, 59–71 (in Chinese, with English Abstract).

Xu, B., Guo, L.Z., Shi, Y.S., 1992. Proterozoic Terranes and Multiphase Collision Orogens in Anhui-Zhejiang-Jiangxi Areas. Geological Publishing House, Beijing (in Chinese, with English Abstract).

Xu, X.S., 1989. Studies on genesis of Precambrian granitoids and their rock inclusions in South China. Ph.D. Thesis. Department of Earth Sciences, Nanjing University, China (in Chinese, with English Abstract).

Xu, X.S., Zhou, X.M., 1992. Precambrian S-type granitoids in South China and their geological significance. J. Nanjing Univ. (Nat. Sci. Ed.) 28, 423–430 (in Chinese, with English Abstract).

Xu, Y.G., 2002. Mantle plumes, large igneous provinces and their geologic consequences. Earth Sci. Front. 9, 341–353 (in Chinese, with English Abstract).

Yan, D.P., Zhou, M.F., Song, H.L., Malpas, J., 2002. Where was South China located in the reconstruction of Rodinia? Earth Sci. Front. 9, 249–256.

Zeck, H.P., Kristensen, A.B., Williams, I.S., 1998. Post-collisional volcanism in a sinking slab setting–crustal anatectic origin of pyroxene-andesites magma, Caldear Volcanic Group, Neogene Alboran volcanic province, southeastern Spain. Lithos 45, 499–522.

Zhao, G.C., Cawood, P.A., 1999. Tectonothermal evolution of the Mayuan assemblage in the Cathaysia Block: implications for Neoproterozoic collision-related assembly of the South China craton. Am. J. Sci. 299, 309–339.

Zheng, J.J., Jia, B.H., Liu, Y.R., Cao, J.H., 2001. Age, magma source and formation environment of mafic-ultramafic rocks in the Anjiang area, western Hunan. Reg. Geol. China 20, 164–169 (in Chinese, with English Abstract).

Zhou, J.C., Wang, X.L., Qiu, J.S., Gao, J.F., 2003. The discovery of Nanqiao highly depleted N-MORB and geological significance. Acta Petrologica Mineralogica 22, 211–216 (in Chinese, with English Abstract).

Zhou, J.C., Wang, X.L., Qiu, J.S., Gao, J.F., 2004. Geochemistry of Meso- and Neoproterozoic mafic-ultramafic rocks from northern

Guangxi, China: arc or plume magmatism? Geochem. J. 38 (2), 139–152.

Zhou, M.F., Zhao, T.P., Malpas, J., Sun, M., 2000. Crustal-contaminated komatiitic basalts in southern China: products of a Proterozoic mantle plume beneath the Yangtze block. Precam. Res. 103, 175–189.

Zhou, M.F., Yan, D.P., Kennedy, A.K., Li, Y.Q., Ding, J., 2002. SHRIMP U–Pb zircon geochronological and geochemical evidence for Neoproterozoic arc-magmatism along the western margin of the Yangtze Block, South China. Earth Planet. Sci. Lett. 196, 51–67.

Zhou, X.M., Zhu, Y.H., 1993. Petrological evidences of Neoproterozoic collision-orogenic and suture belts in southeastern China. In: Li, J.L. (Ed.), Lithospheric Structures and Geological Evolution in Continent from Southeastern China. Metallurgical Industry Press, Beijing, pp. 87–97 (in Chinese).

Zhu, J.C., Li, R.L., Li, F.C., Xiong, X.L., Zhou, F.Y., Huang, X.L., 2001. Topaz-albite granites and rare-metal mineralization in the Limu distract, Guangxi Province, southeast China. Mineralium Deposita 36, 393–405.